ESRF NEWSLETTER

APRIL 1997 EUROPEAN SYNCHROTRON RADIATION FACILITY N° 28

SPECIAL BIOLOGY ISSUE:

In this Newsletter, discover articles on large biomolecular assemblies (p. 12), micro-crystals (p. 15), the «MAD» technique (p. 18 and 21), 3D computed microtomography (p. 26) and the development of an image plate scanner for protein crystallography (p. 30).

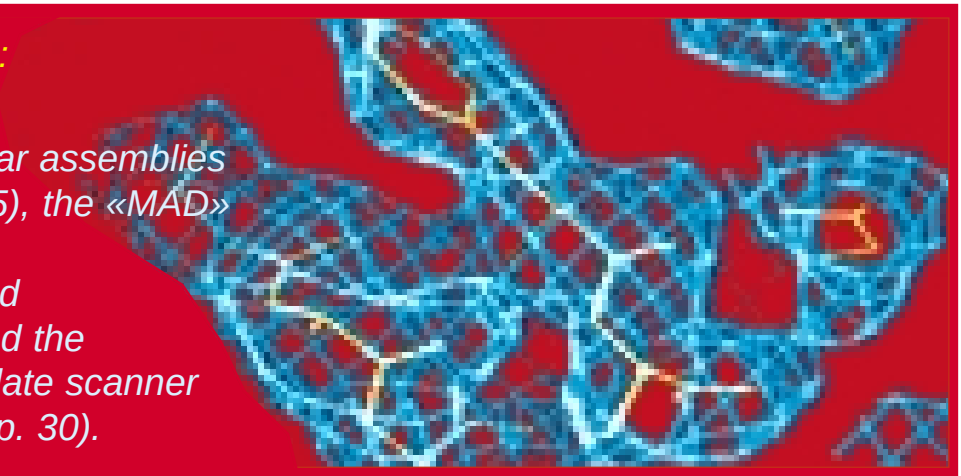

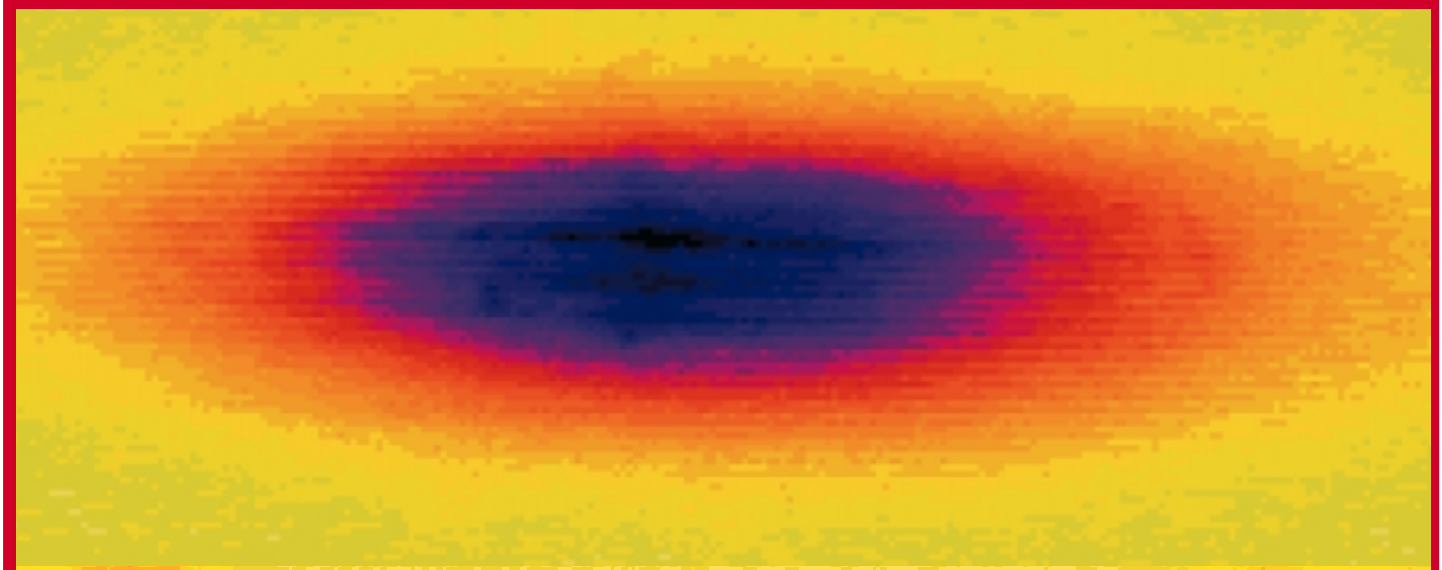

BREAKTHROUGH IN X-RAY OPTICS:

Undulator radiation (top) focused on a spot (bottom) by a refractive lens (p. 33).

ISSN 1011-9310

CONTENTS

Photography by:
C. Argoud, H. Graafsma, C. Jarnias, D. Marshall.

EDITORIAL

A Newsletter on biology

This Newsletter is mainly dedicated to biology, a subject which has hardly appeared in the past issues of the Newsletter. The collaboration between the ESRF and the EMBL Grenoble outstation is now arriving at full maturity and is described on page 10. Papers written by teams from ID2, ID13, BM14, ID19, ID14 and D2AM show the great variety of subjects tackled at the ESRF in the Life Science field.

50 years of synchrotron radiation

Information on the conference «Highlights in X-Ray Synchrotron Radiation Research» organised by the ESRF on the occasion of the celebration of 50 years of synchrotron radiation is to be found on pages 6, 7 and 8 in the documents attached. More information will be given in the next Newsletter due out in July.

ESRF, a gigantic microscope

Please find enclosed a poster «ESRF, a gigantic microscope», which has had a real success amongst our staff and visiting scientists (as well as their families) and that you may also enjoy.

Cybernews

You can now find Newsletter on the ESRF Web Home Page at http://www.esrf.fr. You will also discover the Annual Report 1995/1996 on the Web. It is available on-line only, since it has been decided not to print it.

Information on the conference «Highlights in X-Ray Synchrotron Radiation Research» will also be provided on the Web.

Peter Lindley, New Director of Research

Peter Lindley took over the position of Director of Research on 1 April 1997, in replacement of Carl-Ivar Brändén. Before joining the ESRF, he occupied the position of Assistant Director for Diffraction and Scattering and Head of Life Sciences at Daresbury Laboratory. Among his main responsibilities, he was in charge of the biology programme and the control of project teams in macromolecular crystallography, non-crystalline diffraction and X-ray diffraction. Furthermore, he is a member of a number of scientific societies and co-editor of several scientific journals. His research interests focus on the study of eye-lens proteins, iron and copper metabolism, iron-sulphur proteins and structural biology methods.

APS / SPring-8 / ESRF Workshop

The fourth joint APS/SPring-8/ESRF workshop took place at the ESRF on 7 and 8 April 1997.

A series of 35 fifteen-minutes talks covered a wide spectrum of subjects of mutual interest. During three concluding parallel sessions, topics worth a closer collaboration were identified. For the accelerators these include RF couplers, transverse feedback, RF liners, vacuum conditioning, pinhole cameras and low coupling. Under optics the following items turned out to be of common interest: high heat load material for filters, absorbers, windows; one angstrom smooth mirrors; coherence (measurement, disturbance); diamond supply. For the field of detectors, development and data acquisition, the need of further exchange of information was expressed, in particular as to the comparison of performance and the improvement of user friendliness.

J.M. Filhol, ESRF Machine Director, in discussion with H. Kamitsubo, Director of SPring-8.

Ministers at the ESRF

On Friday 7 February 1997, Charles Millon, President of the Regional Council (as well as French Defence Minister) was joined by François d'Aubert (French Secretary of State for Research) for a tour of the ESRF. About 80 VIPs accompanied the ministers during their visit.

The Swedish Minister of Education and Science, Carl Tham, visited the ESRF on 24 March 1997. He was shown ID11 and ID13 and also met the ESRF Swedish staff.

C. Tham (centre) is showing a strong interest in the explanations given by C.I. Brändén (left).

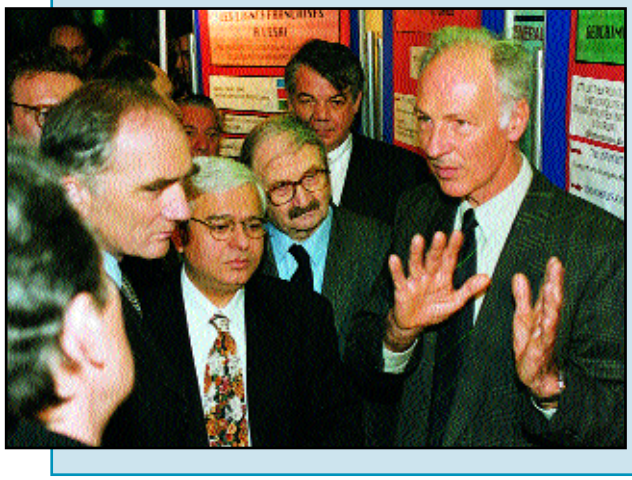

A. Bourret explains the experiments performed at the French CRG IF beamline in front of C. Millon and the accompagnying VIPs.

PARALLEL WORKSHOPS AT «SCIENCE AT THE ESRF»

(1996 ESRF USERS' MEETING)

During the poster session of the workshop on «X-Rays and Magnetism».

WORKSHOP A: X-RAYS AND MAGNETISM

The parallel workshop on «X-Rays and Magnetism» consisted of four sessions: Magnetic X-Ray Scattering, Dichroism in Absorption, Spin Resolved Electronic Structures and Nuclear Resonance and Compton Scattering.

The «Magnetic X-Ray Scattering» session started with a talk of C. Vettier, who first introduced magnetic X-ray scattering techniques, underlining the relevant information brought by non resonant and resonant magnetic scattering; he then showed some new results obtained on different systems. Particular emphasis was given to the reduction of the Pt magnetic moment on the surface of Co_3Pt, to the unsolved problems of the energy dependance of the satellite peaks in Dy films and on the lineshape of the incommensurate phase peaks in UPd_2Si_2.

H. Zabel gave an overview of the present understanding of spin density waves in thin epitaxial Cr layers, showing that spin density waves are almost entirely longitudinal with a Q vector propagating out of plane. A thin ferromagnetic Fe cap layer causes propagation to become transverse and in plane. Sandwiching Cr(001) films between Fe(001) results (via a second reorientation) in an out-of-plane transverse spin density wave with Cr spins now lying in the plane. G. Lander showed a study on the interaction between Fe and Dy magnetic moments in $DyFe_4Al_8$. In this material Fe 3d moments order at T = 170 K, while Dy 4f moments order at T = 20 K. By measuring the $\sigma \rightarrow \pi$ scattering channel at the Dy L edges, it was possible to select the 2p -> 5d dipole transition, thus isolating the 5d Dy magnetic moments: their temperature dependance follows the Fe one, illustrating a relevant 3d - 5d hybridisation in such compounds.

In the session on «Dichroism in Absorption», G. Sawatzky reported on spin resolved photoemission and dichroic X-ray absorption studies of high Tc superconductor antiferromagnets; C. Dalmas de Reotier on the succesfull determination of 5f orbital magnetic moments in $USb_{0.5}Te_{0.5}$, UFe_2 and UNi_2 ferromagnets; C. Meneghini on the correlation between the anisotropic magnetic properties of $CoPt_3$ thin films and the anisotropic Co-Pt local bond distribution.

In the session on «Spin Resolved Electronic Structure», C.F. Hague reported the succesfull observation of XMCD in fluorescence emission spectra on the Rh $L_{\beta 2,15}$ in $Co_{25}Rh_{25}$ alloys; showing the possibility to detect the spin polarisation of valence electrons with this technique; S. Eisebitt on the spin information contained in Fe L_3 fluorescence spectra, which are dominated by the minority spin electrons for the presence of the Auger de-excitation which depresses the spin down channel; H.A. Durr on XMCD and resonant photoemission studies of the 3d electron localisation and exchange coupling of Mn thin films sandwiched with Fe or Ni.

In the session on «Nuclear Resonance and Compton Scattering», Y. V. Shvyd'ko presented the new Nuclear Resonant Small Angle X-ray Scattering technique showing, in the case of α-Fe, how the inhomogeneous magnetisation, namely magnetic domains and walls, can be measured as well as the correlation length and the dispersion of long range spatial variation of magnetisation; R. Lubbers presented some studies of magnetic laves phases at high pressure by Nuclear Scattering; M. Cooper illustrated how Compton Magnetic Scattering determines magnetic moments showing the UFe_2 case in detail, underlining the advantages that the use of ESRF high energy photons provides both in the improvement of momentum resolution and in the data interpretation, when the cross section approaches the Klein Nishima one.

S. Mobilio

WORKSHOP B: CHALLENGING BIOLOGICAL STRUCTURAL STUDIES

The workshop started by giving evidence of the exciting possibilities of ID13 (the Microfocus Beamline, C. Riekel) in providing diffraction patterns from biological crystals of very small size (i.e. couple of tens of microns by dimension) or less organised biopolymers.

H. Belrhali described the experimental arrangement on ID13 set-up by a joint EMBL-ESRF team to permit data collection on protein microcrystals. A 30 μm diameter beam was used and the images were collected on the EMBL 30 cm diameter MAR Research image plate scanner. Several experiments on different systems have been carried out and the crystallographic results presented, demonstrating clearly the feasibility of collecting high resolution crystallographic data sets from such small crystals (see the article from Belrhali *et al.* on page 15).

The different properties of starches depends on the crystalline ultra-structure, which is different according to the origin of starch (type A, cereal starch and type B, tuber starch). In the work reported by A. Buleon it was

shown that with a 2 μm beam it is possible to map the crystallinity and the orientation within a granule of starch with 5 μm step. By using a CCD-image intensifier system, the details of the highly ordered orientation in the structure of type B starch were described in comparison to that of type A starch.

A novel method for the crystallisation of membrane proteins was described by E.M. Landau. It was shown how well-ordered three-dimensional crystals made of membrane proteins can grow in lipidic-cubic phases. Bacteriorhodopsin crystals, not available from micellar systems, were obtained in this way and produced diffraction patterns on ID13 with a significantly higher resolution than previously obtained electron microscopy data.

On the following day, topics focused on time-resolved experiments. The structural modifications undergone by macromolecules with ns time resolution can be recorded by means of fast Laue data collection achieved at ID9 (the White Beam beamline) by using 150 ps X-ray pulses emitted by a single electron bucket from the storage ring. D. Bourgeois described a feasibility study where the structure of native cutinase (a lipolytic enzyme) was refined to 1.5 Å resolution from very fast Laue data and by using as a starting model the structure of mutant R196E. V. Srajer showed the structural changes elicited in carbonmonoxy myoglobin (MbCO) crystals by a 10 ns laser pulse. Photodissociation and rapid (μs) rebinding of CO were described by processing Laue data collected from few ns to 2 μs after the laser pulse.

F. Schotte presented his investigation on membrane protein bacteriorhodopsin (responsible for the photochemical transduction in the purple bacterium) made at ID9 with monochromatic beam and microsecond time resolution. The transient structural change induced on the protein by absorption of a photon was described with unprecedented time resolution.

Defining the structure of the nucleosome core particle (the repeating element in chromatin) is peculiar to investigate gene regulation. Data collected at ID13 and ID9 on an EMBL image-plate by T.J. Richmond made it possible to solve the crystal structure of the nucleosome at 2.8 Å resolution and thus to describe the detailed course of DNA, the structure of histone octamer and its interaction with DNA.

V. Lombardi described combined mechanical and time resolved X-ray diffraction experiments in single intact muscle cells performed at ID2 (SAXS) to investigate the structural changes in the actin-myosin cross-bridges (the molecular motor). With the highly collimated beam at ID2 and with a gas-filled detector placed at 10 m from the specimen, changes in intensity and spacing of the 14.3 nm meridional reflection, sensitive to the movement of the myosin cross-bridges, could be precisely measured with 5 ms time resolution during force development and shortening.

V. Lombardi, G. Belrhali, D. Bourgeois, C. Riekel, S. Cusack

Workshop C: Surfaces and Interfaces

In the «Surfaces and Interfaces» workshop, some of the most significant results obtained in this field at ESRF during the course of 1996 were reported. The title was extensively interpreted: many of the talks reported results in subjects not traditionally included under the label «surfaces and interfaces». Much emphasis was placed on those results which illustrated the new possibilities offered by the ESRF source.

The introductory invited talk was given by S. Ferrer who described recent developments in magnetic surface diffraction. In fact, on ID3, it has been possible to measure the small resonant magnetic signal at the Pt L_3 edge both on the surface of $CoPt_3$ and on the Pt(111) surface covered by a few monolayers of Co; these results extend to the case of surfaces resonant magnetic diffraction, discovered for the bulk in 1988.

Various talks reported new techniques and/or their application. A. Kazimirov described standing waves measurements on thin films of high-Tc superconductors; these measurements exploit, on the one hand, the high flux available on ID32 and, on the other, the element specificity of the technique. The high flux on the same beamline was also used by F. Boscherini to perform standing waves measurements on semiconductor superlattices; the modification of the traditional standing waves analysis in order to obtain the position of specific atoms with respect to the average superlattice planes was also described. Finally, L. Alagna reported Diffraction Anomalous Fine Structure measurements on the superstructure reflections of ordered InGaP/GaAs(001) performed on BM 1 which yielded local structural information on Ga atoms present only in the chemically ordered phase of the InGaP overlayer.

Another group of talks dealt with dynamical processes depending on temperature or time. T. Ressler talked on chemical oscillations during oxidation of CO in the presence of Pt catalysts; measurements were preformed on ID24 using time-resolved X-ray absorption spectroscopy. R. Simon reported specular reflectivity measurements performed on BM32 on Ar thin films deposited on MgO which showed pre-roughnening and layer-by-layer fusion. Two talks dealt with sputtering of semiconductor surfaces, studied by surface diffraction techniques on ID3. The case of CdTe(001) was described by V. Etgens; it was possible to reveal the link between the atomic removal mechanism and temperature and also to show the presence of a strong surface anisotropy. The case of sputtering of Ge(001) was the subject of the talk by D. Smilgies who described changes in the surface dynamic scaling properties with temperature.

Finally, a number of reports tackled problems of considerable complexity with traditional techniques. L. Barbier talked on grazing incidence measurements on vicinal surfaces of a Cu-Pd alloy, describing the «truncation-rod forest» due to the miscut. The growth of Pt on Co(0001), which is highly relevant for magnetic heterostructures, was the subject of the talk by J.P. Deville. Both the talks by Barbier and by Deville were based on surface diffraction measurements performed at ID3. Investigations on the electronic structure of CeRh compounds which used the possibility offered by ID32 of performing resonant photoemission at very high energy (5.7 keV) were reported by D. Chandesris. W. J. Huisman talked on surface diffraction measurements on the rare diamond (111) surface and its interface with liquid Ga; experiments were performed on ID3 and ID10. M. Alba reported diffuse scattering measurements on amphiphilic films performed on BM32 and ID10 which allowed to measure their elastic constants. The structure of grain boundaries in $SrTi_2O_3$ bicrystals was described by J. Zegenhagen using diffraction measurements performed on ID10 and ID11. Finally, the structure of the Pd/MgO interface was the subject of the talk by G. Renaud, using surface diffraction on ID32.

F. Boscherini

HIGHLIGHTS IN X-RAY SYNCHROTRON RADIATION RESEARCH

GENERAL INFORMATION

Fifty years after it was first observed in 1947, synchrotron radiation has become an extraordinary tool for scientific research in a wide range of areas, including "frontier science" as well as industrial research.

"Highlights in X-ray Synchrotron Radiation Research" is an international conference organised by the ESRF in recognition of the pioneering work performed by the first synchrotron radiation users and the remarkable results achieved. It will emphasise the new impetus given to this research by the third generation synchrotron radiation sources in the X-ray range, in fields such as magnetism, high pressure, structural biology, imaging, topography and soft-condensed matter.

Scientific Programme

The scientific programme, from Monday 17 to Thursday 20 November, is made up of plenary lectures given by invited speakers on the above-mentioned topics. These lectures will be followed by poster sessions in the late afternoon. A **call for abstracts** for the poster sessions is enclosed with this Newsletter.

If you do not have it, please complete the pre-registration form below.

Symposium in Structural Biology

The symposium in Structural Biology will take place on 19 - 20 November in the conference centre as a parallel session to the main conference. The symposium will comprise four sessions: «Virus structures», «DNA-replication, transcription, translation and repair», «Time-resolved crystallography» and «Membrane proteins».

Venue

The conference and the annual Users' Meeting (see page 8) will be held at:

ATRIA
WORLD TRADE CENTER
EUROPOLE - GRENOBLE

Dates to remember

Conference date
17-20 November

Structural Biology Symposium
19-20 November

Users' Meeting
21 November

Abstract submission deadline
16 June

Early registration deadline
15 September

We would like to encourage anyone intending to participate in the conference to return the pre-registration form at the bottom of this page in order to receive the next circular due out mid-July. This will contain registration forms for the conference and the satellite meetings as well as accommodation forms. We aim to give those submitting abstracts the date of their poster session at the same time.

Conference Fees

	Before 15 Sept.	After 15 Sept.
Participant	1000 FF	1300 FF
Student	500 FF	800 FF
Accompanying person	500 FF	800 FF
Users' Meeting ONLY (21 Nov.)	250 FF	300 FF

The conference fee includes admission to all scientific sessions and the Users' Meeting, conference documentation and coffee breaks. There will be no published conference proceedings.

Lunch, dinner and the conference banquet are not included in the registration fee. There will be a welcome reception on Thursday 20 November before the Users' Meeting which is included in the fee.

PRE-REGISTRATION FORM

Please return to: SR50 conference secretariat, ESRF BP 220, F-38043 Grenoble cedex, France.
This pre-registration form is also available on the Web at http://www.esrf.fr

In which meetings are you interested?

☐ *Highlights in X-ray Synchrotron Radiation Research and Users' Meeting*

☐ *Users' Meeting only*

☐ *Biology Symposium*

Satellite Meetings

☐ *Magnetic Scattering*

☐ *Topography*

☐ *High Pressure*

Do you intend to present a poster? ☐ Yes ☐ No

Do you want us to send you a call for abstracts?
☐ Yes ☐ No

Please complete in CAPITAL LETTERS

Mr/Mrs/Miss/Dr/Prof
Name: . . . . . .
First Name: . . . . . .

Full postal address: . . . . . .
. . . . . .
. . . . . .
Telephone. . . . . .
Fax: . . . . . .
E-mail:. . . . . .

SATELLITE MEETINGS

The satellite meetings will take place before and after the conference. To date, the following workshops have been planned:

X-Ray Scattering and Magnetism

(Saturday 15 and Sunday 16 Nov.)
Organiser: C. Vettier

Present achievements and future aspirations of X-ray scattering in the physics of magnetism will be discussed during the one-and-a-half-day meeting from both the experimental and theoretical points of view. Presentations will cover such topics as magnetic surfaces, thin films and multilayers, magnetic phase transitions, L and S form factors, resonant scattering, dichroism and absorption, and inelastic scattering. Invited talks as well as poster contributions are planned.

Imaging and High Resolution Diffraction on ID19

(Saturday 22 November
from 9am to 3pm)
Organiser: J. Baruchel

This workshop will focus on the results and possibilities at the long ID19 Topography beamline, mainly devoted to diffraction topography, tomography, phase contrast imaging and high resolution diffraction.

The first users arrived in June 96 and discussion of results obtained and improvements to be made comes at an intermediate date between two "X-Top" meetings. It is a natural follow-on to the imaging round table organised during the Users' Meeting on the 21 November and will consist of two talks and an extended poster session.

Crystallography at High Pressure using Synchrotron Radiation: the Next Steps

(Saturday 22 and Sunday 23 Nov.
with registration on Friday 21 Nov.)
Organiser: D. Häusermann

This workshop is the first meeting organised by the newly formed High Pressure Commission of the International Union of Crystallography, and it will follow the format of the previous IUCr High Pressure Group meetings. The main subject of this workshop will be structural studies and refinement at high pressure using synchrotron radiation, which will include latest developments in high pressure devices, techniques, detectors; data collection and data analysis; and state-of-the-art in powder and single-crystal diffraction, with special emphasis on structure refinement and solution, particularly in extreme conditions of pressure and temperature.

ESRS PRIZE

17-20 NOVEMBER 1997 • GRENOBLE (FRANCE)

On the occasion of fifty years of synchrotron radiation, the European Synchrotron Radiation Society (ESRS) is pleased to announce a prize to be awarded for an outstanding contribution to synchrotron radiation science.
The prize of 1500 ecu will be presented at the International Conference on Highlights in X-Ray Synchrotron Radiation Research organised by the ESRF and co-sponsored by the ESRS in Grenoble, 17-20 November 1997.
It will be given to a person aged 35 years or younger (at the closing date) for work that has been undertaken in Europe after December 1994.
Applicants should send a summary of not more than 2000 words outlining the nature of the research, its significance and their contribution to it, together with any relevant reprints and the names of two referees, to:

Professor C. Norris,
Department of Physics and Astronomy
The University of Leicester, LE1 7RH, UK
Fax +44 (0) 116 252 2770 • e-mail ar@9le.ac.uk

Information can also be obtained from:
http://www.fy.chalmers.se/esrs/welcome.html

Closing date for submission: 1st August 1997

ESRF Users' organisation

USERS' MEETING 1997

20-21 NOVEMBER • ATRIA EUROPOLE

PROGRAMME

Thursday 20 November
20h00 Welcome reception

Friday 21 November
8h30 Coffee
9h00 Introduction
9h10 Directors Report
User Operation
10h00 «Selected User» Talk I
10h40 Coffee Break
11h00 «Selected User» Talk II
11h40 Presentation of the new Council
11h50 Young Scientist Award
12h50 Lunch

14h15 • Parallel Mini-Workshops
X-ray Imaging using Synchrotron Radiation
• Time-Resolved Scattering Techniques using Synchrotron Radiation
• Industrial Applications of Synchrotron Radiation

MINI- WORKSHOPS

Time-Resolved Scattering Techniques using Synchrotron Radiation
Co-ordinator: M. Wulff
21 November 1997

This workshop aims at showing new opportunities in fast diffraction and X-ray spectroscopy techniques on biological and chemical systems. The initiation of fast reactions in macromolecules will be discussed for photosensitive macro-molecules, and laser experts will speculate how ultra-fast X-ray techniques may complement the understanding of the reaction pathway of biological and chemical reactions.

X-ray Imaging using Synchrotron Radiation
Co-ordinator: J. Baruchel
21 - 22 November 1997

Several beamlines at the ESRF devote a substantial part of their time to X-ray imaging. Most of them will be in operation at the end of 1997. The results already obtained and/or the new possibilities in micro-tomography, phase contrast imaging, topography and microscopy will be reviewed and discussed.

Industrial Applications of Synchrotron Radiation
Co-ordinator: J. Doucet
21 November 1997

The workshop is dedicated to the use of synchrotron radiation by industrial companies for research, development or control activities. The diversity of the types of investigations, from long-term fundamental research to urgent requests for characterisation, will be illustrated through presentations given by scientists from several European companies. There will also be open discussions concerning specific access to experimental stations, and how to increase and improve the industrial activity at the ESRF.

YOUNG SCIENTIST AWARD

CALL FOR NOMINATIONS

This nomination form is also available at http://www.esrf.fr/usersorganization/callcand.htm

The Council of the Users' Organisation invites nominees for the 1997 Young Scientist Award. The winner will be named by the Council in October 1997 based on the recommendation of a selection committee appointed by the Users' Organisation chairperson.

Criteria. The award recognises outstanding work done at the ESRF by a scientist 35 years of age or younger at the time of the award.

Nature of award. The winner will be invited to deliver a public lecture at the 1997 ESRF Users' Meeting and will receive a cash award of 5.000 FF.

Everybody, both scientists of the ESRF as well as external users, is encouraged to send in nominations.

Young Scientist Award Nomination Form

Name of the candidate: . . . . . .
Date of birth: . . . . . .
Address: . . . . . .
. . . . . .
Name of the proposer:. . . . . .

State precisely what you regard as the outstanding work accomplished by the nominee: . . . . . .
. . . . . .

What has been his/her contribution to the group effort:. . . . . .
. . . . . .
. . . . . .

What is the relevance of this work to science: . . . . . .
. . . . . .

At which beamline(s): . . . . . **and when**:. . . . . .
did the nominee perform his/her experiments at ESRF.
Please enclose a short CV and a publication list, especially related to the results to be taken into account.

Send it to S. Pascarelli, BP 220, F-38043 Grenoble cedex. e-mail: sakura@esrf.fr
tel. (33) 4 76 88 24 26 • fax (33) 4 76 88 23 25

Users' Organisation: c/o H. Emerich SNBL, P.O. Box220 ESRF F-38043 Grenoble • e-mail user_org@esrf.fr

VACANCIES AT THE ESRF ON 8 APRIL 1997

	Ref	Subject
SCIENTISTS	2179	High energy scattering and imaging
(5-year contracts)	2169	Condensed matter theory
	2192	High pressure beamline
	2203	Troika beamline
	2201	Protein crystallography beamline
	2117	XAFS experiments in the energy dispersive mode
POST-DOC	PDID10A	High brilliance multipurpose undulator beamline (Troika beamline)
(2-year contracts)	PDID15B	High energy X-ray scattering group
	PDID24	XAFS experiments in the energy dispersive mode
	PDID26	X-ray fluorescence excitation spectroscopy on dilute systems
	PDID10B	Troika II beamline
	PDID2	XAFS on the high brilliance beamline
	PDID14A	Protein crystallography beamline
STUDENTS	CFR201	Nuclear resonance
(2-year contract, renewable 1 year)	CFR202	Application of XAS to determine short-range structural properties of liquids
	CFR206	Control of time structure with X-ray optics
ENGINEER	CDD/BPE	Software engineer in the experiments division (18 months contract)
TECHNICIANS	CDD/BPT	3 software support personnel in the experiments division (18 months contract)
	1513	Radiation protection

If you are interested, please send us a fax (+33 (0) 4 76 88 24 60) or an e-mail (peritore@esrf.fr) with your address, and we will provide you with an application form. You can also print out an application form on the World Wide Web http://www.esrf.fr

JOINT STRUCTURAL BIOLOGY GROUP BETWEEN EMBL AND ESRF

The intense and highly collimated X-ray beams at the ESRF are ideal for studying the generally weak diffraction from large biological macromolecules. Therefore structural biology has become one of the major applications at the ESRF: six ESRF beamlines are concerned with structural biology (**Table 1**).

Some five years ago, in mid-1992, the ESRF and the EMBL approved a Memorandum of Understanding on the use of synchrotron radiation for biology research. This memorandum provides for formal specific agreements to be discussed and implemented covering beamline design and construction and the collaborative use of EMBL, ILL and ESRF facilities (cf. ESRF Newsletter N° 15, p. 3). Since then extensive interactions between EMBL and ESRF have been developed concerning beamline design, construction and operation, development and testing of new equipment, in-house research as well as safety issues.

In order to optimise the use of the facilities we have established a more structured and coherent framework for the collaboration in the form of a Joint Structural Biology Group (JSBG). This group was formally approved by both ESRF and EMBL Councils late last year.

The group is managed by two scientists from the two institutes, who alternate between being head and deputy head of the group. The group acts in a similar way as other ESRF groups in that it co-ordinates the activities of several beamlines which share common scientific interests. At present, the number of JSBG members is about 40 including associate members who formally belong to other groups.

The combination of the "Institut Laue-Langevin" (ILL), the "Institut de Biologie Structurale" (IBS), the EMBL Outstation, and the ESRF has made Grenoble a unique place for structural biology and the JSBG will hopefully play an active role in enhancing this further. The details of the group structure and responsibilities are being finalised with an emphasis on facilitating interactions and information flow among the protein crystallography beamlines and the EMBL groups. The objectives of the group are as follows:

DEVELOPMENT PROJECTS

There are many aspects common to all the JSBG beamlines: (1) beamline components such as collimators, beamstop, cryocooling, and alignment system for small crystals, (2) CCD and Imaging Plate detectors, (3) beamline control with graphical user interface, and (4) general computing environment for processing extremely large volumes of data. One of our aims is to co-ordinate the protein crystallography beamlines to present a similar environment to the users and assist the beamline staff to pursue new technical developments. Currently, there are a number of joint projects such as automatic beamline alignment, storage and transfer set-up of frozen crystals, sample observation devices for micro-crystals, pressurised Kr/Xe cells for phasing, a 40 cm by 80 cm imaging plate drum scanner for beamline ID14 and a rapid imaging plate changer for beamline BM14. Different project teams are formed across the beamlines according to the nature of the projects and their results are reported and discussed in the regular group meetings.

IN-HOUSE RESEARCH PROJECTS

Almost every research project in structural biology requires a large amount of laboratory work to obtain crystals for X-ray studies using biochemical and molecular biology techniques. The ESRF does not have the facilities for such experiments but, under the framework of the JSBG, ESRF scientists have an option of working independently in a laboratory at EMBL, establishing outside collaborations or joining an EMBL research group. Several such projects have already started. The long-term aim is that the JSBG will nurture challenging and front-line scientific projects which require a wide range of expertise in molecular biology as well as beamline instrumentation.

WORKSHOPS

Following the success of the EMBL/ESRF/IBS workshop on multiwavelength anomalous diffraction (MAD) in June 1996, the JSBG is organising a second workshop on the MAD technique in June 1997. This will be extended to other subjects in protein crystallography including training courses in data collection and data analysis.

Table 1: ESRF beamlines concerned with structural biology.

Beamline	*Time dedicated to structural biology*	*Operation since*	*Specific applications*	*Detectors*
ID2 (PX)	*half*	*Sept 1994*	*monochromatic protein crystallography*	*IP*
ID9	*half*	*Sept 1994*	*time-resolved Laue, monochromatic protein crystallography, trapping of intermediates*	*CCD, IP*
ID13	*one third*	*Sept 1994*	*micro crystals*	*CCD, IP*
ID14 A/B			*monochromatic protein crystallography*	
EH1	*full*	*1998*		*CCD*
EH2	*full*	*1998*		*CCD*
EH3	*full*	*Sept 1997*	*large proteins and viruses*	*IP, CCD*
EH4	*full*	*Sept 1997*	*multiwavelength anomalous diffraction (MAD)*	*CCD*
BM14	*full*	*Sept 1995*	*multiwavelength anomalous diffraction (MAD)*	*CCD, IP*

"Test beam time"

It has been suggested by a number of user groups and the Life Science beam time allocation Review Committee that it would be extremely useful if the ESRF provides "test beam times" for users to test newly-grown crystals to see how well they diffract before making a formal beam time proposal. At Stanford Synchrotron Radiation Laboratory, this has already been put into practice. The JSBG will assist beamline scientists to organise such test beam time shifts on selected beamlines.

Sample preparation

At the moment, there are two sample preparation areas close to ID2 and on BM14. There is a plan to build another for ID14A/B. These will be maintained by the JSBG to give users useful space to prepare crystals before and during their beam time. More extensive biochemical facilities are of course available for users at the EMBL.

There is also a plan to equip one of the four experimental stations of ID14 with a P2 level facility for biohazardous experiments such as virus crystals. It consists of a laminar flow enclosure around the kappa diffractometer, and another laminar flow hood next to the experimental station to minimise the risk of accidents during the transfer of virus crystals. The safety aspect of the project is overseen by an EMBL scientist who assists the ESRF Safety Group and the beamline staff.

Working groups

Working groups are formed in order to address global projects common to the JSBG such as the ESRF biochemistry laboratory, tapered optics fiber coupled CCD detectors, management of computer systems of JSBG beamlines, decision of in-house research projects and co-ordinated development of new projects. These groups have well-defined goals and time schedules for completion of the projects.

Collaboration with the IBS in Grenoble

Currently, three scientific collaborators from the IBS (Institut de Biologie Structurale) collaborate with the JSBG members in the design, construction and operation of the ESRF protein crystallography beamlines. They act as liaison between the JSBG and the IBS in instrumentation and structural biological projects as well as workshops. For instance, BM14 and the CRG beamline D2AM benefited from the exchange of ideas on the use of the ESRF X-ray Image Intensifier CCD detectors. A possibility of forming a thematic group on structural virology is being discussed among IBS, EMBL, ESRF and other virology groups in the Rhône-Alpes region.

HERCULES 1997

The seventh session of the HERCULES course (Higher European Research Course for Users of Large Experimental Systems) took place at the Maison des Magistères, CNRS Grenoble, from 16 February to 27 March 1997 with 82 participants from 18 countries (mostly European, but including participants from Brazil, China and Japan who are registered at European Universities):

- session A: neutron and synchrotron radiation for physics and chemistry of condensed matter with 44 full-time participants and 19 part-time participants.
- session B: neutron and synchrotron radiation for biomolecular structure and dynamics with 19 full-time participants.

As in previous years, the course included lectures, practicals and tutorials. This year, session A was particularly centered on recent developments of neutron and X-ray spectroscopy (circular magnetic dichroism, inelastic scattering...). In Grenoble, most of the practicals were carried out at ESRF beamlines (including French, Italian and Swiss-Norwegian CRG beamlines) and at the ILL. The collaboration of EMBL, IBS as well as CNRS and CEA-Grenoble was also greatly appreciated. Participants from the two sessions carried out practicals at LURE (Orsay) and the Léon Brillouin Laboratory (Saclay).

The poster session at the Maison des Magistères (54 posters displayed) was one of the highlights of the course and allowed fruitful exchanges between participants and Grenoble scientists.

HERCULES 98 will take place next year with the same two parallel sessions, from 22 February to 3 April (provisional dates).

Information and application forms will be available at the beginning of July 1997.

From left to right, front row: P. Bösecke, J. Gorini, O. Diat, B. Rasmussen, J. Lescar. Back row: J.M. Bois, D. Pognant, F. Felisaz, F. Lapeyre, J. Grimes, E. Mitchell.

ID2: A Brilliant Source for Probing Large Biomolecular Assemblies

J. Lescar[1], E. Mitchell[1], J. Gorini[1], O. Diat[1], P. Bösecke[3], J. Grimes[2], J.-M. Bois[2], F. Felisaz[2], L. Claustre[2], D. Pognant[2], F. Lapeyre[2] and B. Rasmussen[2]

1 ESRF, Experiments Division
2 EMBL, Grenoble Outstation
3 Max Planck Institut, Hamburg

The cell is an amazingly complex system of interacting macromolecules. One of the major challenges in the structural molecular biology of today is to understand how complex integrated systems function, in a dynamic way, within the living cell. Instead of studying individual biomolecules as separate pieces, there is a need to address structural problems which involve assemblies composed of many biomacromolecules (generally proteins in association with lipids, sugars, or nucleic acids) and with total molecular weights superior to 100 kDa and up to tens of MDa. Surprisingly, such enormous systems can be well ordered and can give rise to near atomic resolution structures. Conversely, on a smaller scale, increasing numbers of ab initio drug design programs require the collection of very high resolution data for single proteins which are important pharmaceutical targets.

Large bio-assemblies tend in general to give only tiny crystals with volumes less than 10^5 mm^3, even after years of crystallisation trials. Such crystals diffract very weakly and adequate data cannot be collected using conventional X-ray sources. This has hitherto prevented structure determination of important biological systems like membrane proteins.

Furthermore large macromolecular assemblies yield crystals with large unit cells (some virus crystals have unit-cell parameters up to 1500 Å). These sample peculiarities require both a high photon flux through a small cross-section and also an essentially parallel beam. With such characteristics, the many closely-spaced spots from a large unit-cell crystal can be resolved and a good signal-to-noise for weak reflections can be obtained.

The High Brilliance beamline ID2, with a highly collimated undulator source, ideally fulfils the requirements for crystallography of biological complexes. ID2 provides one of the most brilliant X-ray source for Macromolecular Crystallography in the world and was one of the first ESRF beamlines to become operational in September 1994. The beamline is devoted to macromolecular crystallography experiments for half of the usable time, the other half being devoted to small-angle scattering (including on biological samples such as muscle fibres) on the second end-station. ID2 is equipped with two undulators (46 mm and 26 mm) which produce a small (100 x 100 μm) parallel beam with a flux of about 6 x 10^{12} ph/s/100 mA through the sample.

In addition, two cryocooling devices (Oxford Instruments Cryostream and a coaxial FTS system) allow regulation of the sample temperature between 100 K and 293 K. Data collection at low temperatures, preferably at 100 K if the crystal can be frozen, is essential to avoid radiation damage and obtain more accurate measurements. A five-circle Huber diffractometer with a long 2θ arm allows positioning of the detector up to 1m away from the crystal. This allows diffraction spots from crystals with very large unit cells (up to 1500 Å for crystals containing whole viral particles) or large mosaicity (which was the case for the membrane protein Photosystem I) to be resolved. In addition, the 2θ arm can also be swung (± 20 degrees) allowing high resolution data to be collected even at long crystal-to-detector distances.

Table 1

Viruses	
• *Small RNA bacteriophages*	*Liljas et al. (1996) Structure 4 543-554*
• *Structure of Blue Tongue Virus*	*Stuart et al. (1997) In preparation*
Drug design	
• *HIV-I Reverse Transcriptase*	*Stuart et al. (1995) Structure 3 915-926*
• *Isopenicillin Synthase*	*Hajdu et al. (1995) Nature 375 700-704*
• *HIV Protease*	*Lescar et al. (1997) J. Mol. Biol. In the press (collaboration with Institut Pasteur Paris)*
Membrane proteins	
• *Structure of photosystem I*	*Krauss et al. (1997) Nature Struct. Biol. 3 965-973*
• *High resolution studies of the light-harvesting complex from photosynthetic bacteria*	*Freer et al. (1997) In preparation*
• *Structure of cytochrome c oxidase at 2.8 Å resolution*	*Iwata et al. (1995) Nature 376, 660-669*
Nucleic acid-protein interactions	
• *Crystallographic studies on ribosomes*	*Yonath et al. (1996) Structure 4 513-518*
• *Aminoacyl-tRNA synthethases and their tRNA complexes*	*Cusack et al. (1996) EMBO journal 15 6351-6334*

A number of structural biology projects, including complete virus particles, targets for drug-design, membrane proteins and nucleic acid-protein complexes have made use of the beamline (some of them are listed in Table 1). For many systems ID2 has provided the experimenters with data to higher resolution than previously achieved, allowing a more detailed understanding of fundamental biological phenomena, for example viral replication or plant photosynthesis. Of the many demanding projects that were successfully carried out over the past two and a half years of operation, we have selected four examples to illustrate how a high brilliance X-ray source can be utilised to probe and understand large biological assemblies.

VIRUSES; BLUE TONGUE VIRUS

Understanding viruses that infect cattle and how to combat them

Blue Tongue Virus (BTV), an orbivirus, is a member of the Reoviridae family and infects ruminants and domestic cattle, causing diseases of great economic importance. The Blue Tongue Virus project has been described in some detail in the ESRF Highlights 1995/1996. We would like to summarise the overall status of this project. The virus particle is very large in structural terms (800 Å in diameter and with a molecular weight of 60 MDa) and is composed of 4 capsid proteins (with differing copy numbers ranging from 120 to 780) and 10 unique double-strand ribonucleic acids, each associated with its transcription complex (made up of 3 or 4 proteins). Core particles, with the two outer capsid proteins removed, have been crystallised by D. Suart's group at Oxford and diffraction data have been collected at ID2 on several occasions. These data to 3.5 Å resolution could not have been collected at any other beamline. The Blue Tongue Virus project is probably the largest biological assembly giving well-diffracting and interpretable diffraction data and a near atomic resolution structure (3.5 Å).

HIV1-REVERSE-TRANSCRIPTASE (RT)

Improved drug design to prevent AIDS?

The genome of HIV (the causative agent of AIDS) encodes three enzymes, each with an essential function in the infectious cycle of the virus. One of these enzymes, the reverse transcriptase or RT, is responsible for the conversion (transcription) of the viral genome into DNA molecules which are then incorporated into the host-cell genome. As a crucial element in the infectious cycle, this enzyme has been the primary target for antiviral therapy, and analogues of the building blocks of DNA such as AZT or DDI have been used as tentative AIDS therapeutic agents because they bind to RT and prevent its function. Several mutations however have been observed within the RT molecule, which enable it to escape the binding of these drugs. Detailed structural information of mutated forms of the RT molecule are needed in order to understand the way these mutations allow the RT to escape binding of existing drugs and to help design others. Since RT is a large enzyme containing several subdomains linked by flexible segments, crystals have been extremely difficult to produce and usually diffract poorly.

The technical characteristics of ID2 have helped the Oxford group to collect higher resolution data on these projects and produce a clearer understanding of this enzyme.

MEMBRANE PROTEINS; PHOTOSYSTEM I

Understanding plant photosynthesis

Photosynthesis is the process whereby solar light energy is converted into a chemical form readily available to living systems. Two groups of plant photosystems (numbered PSI and PSII according to the nature of their terminal electron acceptor: either an iron sulphur cluster or a quinone molecule) have been extensively studied through biochemical, spectroscopic and structural methods. The large chlorophyl antenna of PSI capture and channel excitation energy to the primary electron donors (chlorophyl molecules) located near the light-sensitive side of the membrane, which further transfer the electron to Fe_4S_4 clusters. On the basis of data collected on ID2 to 3.8 Å resolution, which have been recently extended to 3.5 Å resolution, the geometry of the cofactors, which are important structural elements within the electron transfer chain, could be imaged

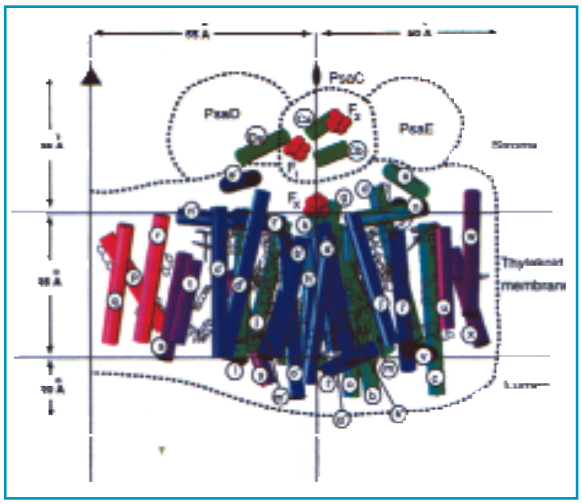

Fig. 1: (from Krauss et al., Nature Struct. Biology, 3, 965) Overall view of the photosynthetic system I molecule - Courtesy of N. Krauss, Institut für Kristallographie Berlin, Germany) α-helices are represented as tubes and labelled a-y. Transmenbrane and surface α-helices of the peripheral subunits are purple, those involved in trimerisation red, those of the extrinsic stromal subunits are green. The porphyrin headgroups of chlorophyll a are indicated as wire models, atoms of iron-sulphur clusters as red spheres.

much more precisely (Figure 1). The fine collimation of the beam provided by ID2 proved to be essential for resolving broad spots due to a large mosaicity of the crystals. This structure determination has provided a basis for understanding photosynthetic reaction centres involving iron sulphur clusters. Furthermore, this result has an interesting implication for understanding the evolution of photosynthetic systems within plants: despite a low level of primary sequence homology (the sequence of amino-acids of the two PS bear no obvious resemblance), structural analogy between PSI and PSII indicates that these two classes of photosynthetic systems may derive from a common ancestral molecule.

NUCLEIC ACID-PROTEIN COMPLEXES

Understanding the basic machinery of life: protein biosynthesis

Proteins are the «workhorses» of the living cell: they are used as enzymes to catalyse metabolic reactions, as antibodies to protect higher organisms against pathogens, as structural motors and as signal transducers between the outside of the cell and the nucleus which stores the genetic information.

The way genetic information is specifically translated into proteins depends in part upon specific interactions between nucleic acids and protein molecules. In order to elongate the growing polypeptide chain with the correct amino acid, one important step is the correct attachment of cognate amino acids onto their cognate tRNA molecules, which is catalysed by specific enzymes called tRNA synthetases. Much work has been done at the EMBL in Grenoble by the group headed by S. Cusack to understand the structural basis of these interactions. ID2 has enabled high-resolution structure determination of several aminoacyl-tRNA synthetases and their complexes with cognate tRNA (Table 1). Protein biosynthesis is carried out by numerous enzymes, tRNAs and other protein factors which act in concert with a macromolecular complex called the ribosome, where the synthesis of the growing polypetide actually takes place. This «factory» consists of many proteins (up to 73) and several RNA molecules which ensure a coordinated translation of the genetic code. Several crystals from different ribosomal systems have been grown and are being characterised by the group of Dr Yonath at Hamburg and at the ESRF on ID2. Together, through obtaining better images of these macromolecular assemblies, this work opens the way to a better understanding of the mechanism and the interactions crucial for the protein biosynthesis machinery.

Reference

N. Krauss, W.-D. Schubert , O. Klukas, P. Fromme, H.T. Witt, W.. Saenger(1996) Photosystem I at 4 Å resolution represents the first structural model of a joint photosynthetic reaction centre and core antenna system. Nature Struct. Biol. 3, 965-973.

CRYSTALLOGRAPHY WITH BIOLOGICAL MICRO-CRYSTALS

H. BELRHALI[1], A. BRAM[1,2], S. CUSACK[3] AND C. RIEKEL[1]

1 ESRF, EXPERIMENTS DIVISION
2 SIEMENS MICROELECTRONICS CENTER GMBH, GERMANY
3 EMBL GRENOBLE OUTSTATION C/O ILL, GRENOBLE

From left to right: S. Cusack, C. Riekel and H. Belrhali.

Crystals of biological macromolecules are produced from solution by decreasing the solubility of the macromolecules often by using a «precipitant». Crystallisation of biomacromolecules is still as much an art as a science and if the first hurdle is to get any crystal at all, the second hurdle is to get a crystal of sufficient quality and size for crystallographic data collection.

This is required because the intensity I_{hkl} of a diffracted ray by a crystal is proportional to the ratio of its diffracting volume V_χ to its unit cell volume V_c and also to the incident beam intensity I_0:

$$I_{hkl} \propto (V_\chi / V_c) \times I_0$$

For macromolecules, V_c is generally large (typically $10^6 Å^3$) and the total diffracted intensity is split up into many hundreds of weak reflections. Crystals used for most biocrystallographic experiments on standard synchrotron sources therefore need to be typically a few hundred micrometers in linear dimensions. However it is often much easier to obtain micro-crystals up to a few tens of microns in size. The highly focussed intense undulator beams available on third generation synchrotron radiation sources now permit good quality data to be obtained on such previously unusable crystals.

In order to test this approach we have used the Microfocus beamline (ID13) with the aim of obtaining complete high resolution data set collections on micro-crystals. The high flux density of the Microfocus beamline is particularly adequate for these studies but the associated problems of sample manipulation, visualisation and sample stability need also to be addressed.

As shown in Figure 1, the flux density at the sample position can be increased by focusing the beam. The focusing element on ID13 is an ellipsoidal mirror which produces a beam of approximately 30 μm with a gain factor of $\geq 7 \times 10^3$ as compared to a collimated beam. In the case of larger crystals, a microfocused beam could also be used as a probe to screen perfect sub-volumes or to irradiate fresh parts of crystals. The principle of the method is also shown in Figure 1.

INSTRUMENTATION

Experiments were performed with a monochromatic beam (Si-111) at a wavelength of 0.688 Å. The beam divergence at the sample position was 2.3(h)x 0.44(v) mrad^2. The estimated flux in the 30 micron beam at the sample position was about 5×10^{10} photons/s when the synchrotron was operated in the 16-bunch mode. Under optimal conditions the flux can become $>10^{12}$ photons/sec.

The precise ID13 Nonius κ-goniometer was used for the experiments. A 30 cm MAR image-plate detector was installed and synchronised with the SPEC instrumental control system. Samples, held in tiny loops, were cooled to 100° K by an Oxford Cryostream® system. Crystals were optically centered on the goniometer by a QUESTAR® long-distance microscope. Fine tuning of the sample position in the beam was done in real time by observation of the diffraction pattern using an "X-ray eye" CCD camera. Translation of the whole goniometer, with micrometer precision, was also used to expose fresh volumes in the case of large crystals.

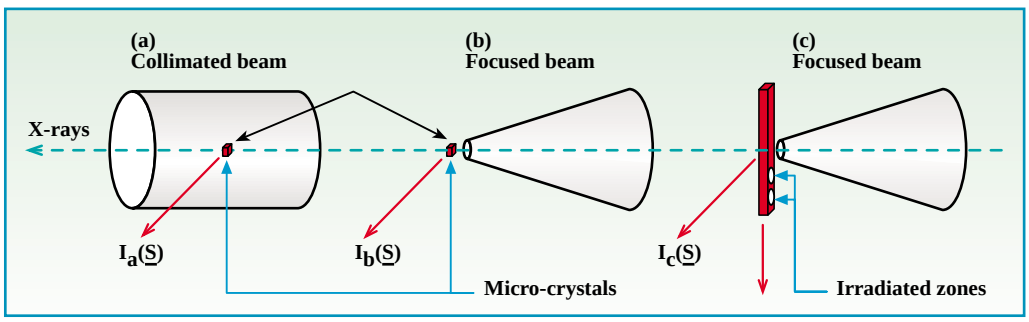

Fig. 1: Intensity I(S) diffracted from a micro-crystal in (a) a collimated and (b) a focused X-ray beam and (c) by a macro-crystal in a focused beam.

Macromolecules	Histidyl-tRNA synthetase + Histidine + AMPCPP+Mn++	Asparaginyl-tRNA synthetase	Prolyl-tRNA synthetase + tRNAPro	T Protein:DNA	p52:DNA	Bacteriorhodopsin	HIV-1 p24:fab
Space group	P21212 (Orthorhombic)	P6422 (Hexagonal)	P4X212 (Tetragonal)	P212121 (Orthorhombic)	I212121 (Orthorhombic)	P63 (Hexagonal)	C2 (Monoclinic)
Cell parameters (Å, Å, Å // ß°)	175, 215, 49	125,125,123//120	143,143,231	39,113,147	45,129,132	62,62,104//120	194,48,191//92.4
Crystal dimensions (mm^3)	40x40x100	30x30x50	100x100x100	100x100x80	500x80x50	30x50x5	100x100x20
Resolution limit (Å)	~2.9	~ 2.3	~ 3.5	≥ 2.00	~ 3.8	≥ 2.3	~ 4.0
Comments	92 % complete Rsym = 9.0 %	80 % complete Rsym = 15 % 3 translations	rapid decay 4 images	78 % complete Rsym = 8.4 % 2 translations	80 % complete Rsym = 8.0 %	91 % complete Rsym = 10.5 %	86 % complete Rsym = 12 %
Experimenters	H. Belrhali (ESRF) A. Yaremchuk (EMBL)	C. Berthet -Colominas L. Seignovert (EMBL)	S. Cusack, A. Yaremchuk (EMBL)	C. Müller (EMBL)	P. Cramer, C. Müller (EMBL)	E. Pebay-Peyroula (IBS), E. Landau and G. Rosenbusch (BIOZENTRUM)	C. Berthet-Colominas S. Cusack (EMBL)

Table 1: Macromolecule micro-crystals used on ID13 (beam size = 30 µm ϕ , λ = 0.6883 Å).

EXPERIMENTAL RESULTS

Using the experimental set-up described above, a number of interesting biological crystals have been examined (see Table 1). Most of the experiments, except the one with prolyl-tRNA:$tRNA^{Pro}$ complex, led to usable data comparable in quality to data sets recorded on other beamlines, if not better. This is particularly true for the bacteriorhodopsin project, where for the first time ever three-dimensional crystals were measured to high resolution giving data from which a 2.5 Å crystal structure has been determined. Exposure times per image were of the order of 60 seconds. We note that patterns of comparable intensity require a 100 µm beam on ID2. This could be further improved by increasing the number of undulator segments on ID13.

In the case of the T protein: DNA complex project, the available crystals were mosaic. The use of the microfocused beam allowed the screening for more perfect sub-volumes of those crystals, allowing the collection of a complete high resolution data set. Similarly in the case of the HIV-1 p24/Fab complex, single crystal regions of a macroscopically twinned crystal could be picked out.

The price to pay for the high flux density is a faster radiation damage of the crystals even at cryo-temperatures. Most of the samples showed a shorter lifetime in the beam compared to previous experiments performed on beamlines with less flux density. Larger crystals were systematically translated during the data collection in order to expose fresh volumes.

PERSPECTIVES

The results described above are very promising. However, before micro-diffraction on biological crystals becomes a routine technique, several points have to be addressed systematically.

Micro-crystal manipulation

It is indeed very difficult to "fish" micro-crystals using the classical stereo zoom microscopes. Higher resolution microscopes and alternative ways of fishing the crystals have to be explored, perhaps using micro-manipulators.

Sample observation

We encountered difficulties in the handling of very small crystals and in particular to observe them clearly while centering on the goniometer. In the frozen droplets, the crystals are extremely difficult to distinguish not only because of their size but also because of the frozen mother liquor droplet that surrounds each of them and produces light reflections. We are presently exploring the use of crossed polarizers in order to enhance the visibility.

Sample lifetime

The lifetime of the crystals in the beam has to be increased. Lower temperatures and/or shorter wavelength could be explored. However it could be that the intrinsic limit due to primary radiation damage is being reached.

Detector

A large area CCD detector would increase the data collection rate, and therefore would permit a complete data set to be collected in a shorter time and allow at the same time ϕ-slicing to improve the signal-to-noise ratio. We aim to install a 2000 x 2000 pixel CCD detector with a read-out time of less than 10 seconds. In contrast the read-out time of the 30 cm diameter MAR image plate is about 200 seconds!

CONCLUSION

We have demonstrated the feasibility and utility of protein micro-crystal diffraction on ID13. For problems in which there are only micro-crystals (for example bacteriorhodopsin), ID13 now makes crystal structure determination possible. Development of appropriate tools for sample observation, manipulation and storing is required.

ACKNOWLEDGEMENTS

The hardware and software were set up by a combined EMBL-ESRF JSBG team. The authors would like to thank many people who have contributed to this project, i.e., C. Berthet-Colominas, J.-M. Bois, M. Chiu, L. Claustre, P. Cramer, P. Engstrom, S. Fiedler, F. Felisaz, E. Landau, F. Lapeyre, S. Monaco-Malbet, C. Müller, E. Pebay-Peyroula, D. Pognant, V. Rey Bakaikoa, G. Rummel, L. Seignovert, M. Tukalo, S. Wakatsuki, P. Wattecamps and A. Yaremchuk.

D2AM-BIO: STEPS TOWARDS BETTER PROTECTION OF TOBACCO CROPS AND NEW DESIGN OF ANTIBIOTICS

G. BOISSY[1], S. BRUNIE[1], J. BERTRAND[2], E. FANCHON[2], O. DIDEBERG[2], M. ROTH[3] AND J.-L. FERRER[3]

1 UNITÉ DE RECHERCHE BIOCHIMIE ET STRUCTURE DES PROTÉINES, INRA, JOUY-EN-JOSAS (FRANCE)
2 LABORATOIRE DE CRISTALLOGRAPHIE DES MACROMOLÉCULES, IBS, GRENOBLE (FRANCE)
3 LABORATOIRE DE CRISTALLOGRAPHIE ET CRISTALLOGENÈSE DES PROTÉINES, IBS, GRENOBLE (FRANCE)

Many protein structures were solved in 1995 and 1996 with data collected on D2AM, the CRG beamline on the bending magnet BM2. A new cytochrome structure, mutants of a hydrogenase, β-lactamase, structures of molecular complexes, such as protein-inhibitor (psychrophylic amylase) or protein-cofactor (17β HSD) complexes were determined using essentially molecular replacement. Three structures were solved ab initio with multiwavelength anomalous diffraction (MAD) data collected at the Pt, Se or Fe absorption edge. The first two, *cryptogein and MurD*, will be presented below; the refinement of the third one, a new form of cytochrome c3, is currently in progress at 1.7 Å resolution. The beamline was also successfully used for mosaicity measurements on protein crystals grown in microgravity, the angular resolution of these measurements being of the order of 3.

These results demonstrate the great flexibility of use of the D2AM beamline for protein crystallography. Instrument and software allow one to collect easily diffraction data at n wavelengths, where n can be 1, 2, 3 ... or up to 20 values, at any temperature between -180°C and room temperature. In addition, these results also demonstrate the good quality of data obtained with the XRII-CCD detector and evaluated with XDS [1]. As an example, a lysozyme data set collected at 2Å, the diffraction limit of the crystal, showed an R_{sym} of 2.5%.

AN ORIGINAL 3-D PROTEIN STRUCTURE

Fungi of the genus Phytophthora are a major natural cause of crop devastation. For example, they are responsible for the blight of potatoe plants (*Phytophthora infestans*) which destroyed the potato crop in Ireland in 1845 causing the great starvation which is at the origin of the massive emigration of Irish to the United States, and the mildew of vineyards (*P. vignae*) which destroyed the French vineyard at the beginning of the century, or the black shank of tobacco plants (*P. parasitica* var. *nicotianae*). Even nowadays one third of the world tobacco production is damaged by this infection. The baleful action of the fungus is due to the invasion of the roots and stalks of the plant by the mycelium of the fungus producing the lethal perishment (Figure 1). However most species of the *Phytophthora* fungi family do not have such a catastrophic effect on the plant they infect, but they induce only localised necrosis of leafs. In effect most of these fungi secrete a small molecule called *elicitin* and plants have developed a system of defence against fungal invasion, which is triggered off by this molecule. The localised necrosis of the leaf can be considered as a manifestation of this defensive response. One may think for instance that the plant destroys the locally infected tissue. The virulence of the few fungi, which induce a lethal pathogenicity, like *P. parasitica* on tobacco, is due to the absence of elicitin by these fungi. They have the particularity of not having elicitin secretion. The reactivity of plants to elicitin is not very specific. Once the plant

Fig. 1: a tobacco plant infested by the fungus Phytophhtora parasitica nicotianae. Cryptogein, a protein secreted by Phytophhtora cryptogea, a fungus belonging to the same family, induces an immunisation of tobacco plants against P.p.nicotianae. The toxicity of the protein produces nevertheless a non lethal localised necrosis of the plant.

has acquired this mechanism of defence by contact with an elicitin, it is protected against any further fungal invasion, even by a fungus of *Phytophthora* family which do not have elicitin. This was demonstrated by injecting elicitin to tobacco plants and testing afterwards their resistance to infection by *P. parasitica*. The analysis of the properties of the elicitins shows first that they belong to two classes, highly necrogenic elicitins and less necrogenic elicitins, the later being 50-100 times less necrogenic than the former, and secondly that necrogenicity and ability to activate the plant defence mechanisms are not correlated. This evidence allows one to imagine new approaches for agricultural fungicid developments based on elicitins. It might be possible to engineer an elicitin, non-necrogenic but powerful for protecting plants. To achieve this end, it is necessary to know first in great details the structure of the molecule and the characteristics of this structure which explain its properties.

All members of the elicitin family identified up to now have very high sequence homology. They constitute a *new family of proteins*. No primary sequence homology with any other known protein was found. The comparison of the sequence of the highly necrogenic elicitins and the less necrogenic ones has allowed to select several potential necrotic activity-determining residues. But it seems that the residue at position 13 plays a key role in this property. It is a lysine in the highly necrotic elicitins and a valine in the less necrotic elicitins. This was demonstrated by replacing Lys13 by a valine by site-directed mutagenesis. The mutation produced a dramatic alteration of the necrogenicity of the protein. In order to identify more structural features important for the necrotic activity of elicitins, the crystallographic structure determination of cryptogein (CRY), secreted by *Phytophthora cryptogea*, was undertaken.

In collaboration with the Laboratory of Dr. Pernollet (INRA, Jouy-en-Josas, France), CRY was crystallised in high salt concentration (4.9 M NaCl) in space group $P4_122$ (a = b = 47 Å, c = 137 Å). The absence of sequence homology with structurally characterised proteins directed efforts towards the isomorphous replacement method. The extensive search for heavy-atom derivatives yielded only one poorly phasing tetrachloroplatinate derivative, with a rather low atomic occupancy. This difficulty might be related to the unusual property of the molecule which lacks for several amino-acids which are important for heavy atom binding like His, Glu, Arg. The six cysteines found in the sequence are involved in disulfide bridges. The crystal structure was therefore solved by the multiwavelength anomalous diffraction phasing method. Four data sets were collected in the vicinity of the platinum LIII absorption edge ($\lambda \approx 1{,}0723$Å). A native data set was collected in addition for completion. In the first stage, the MAD platinum derivative data were phased using the programs MLPHARE [2] or HEAVYv4 [3]. The resulting electron density map was interpretable but its overall quality was not good enough for a clear identification of all secondary structural elements, even after solvent flattening by the program DM [2]. In contrast, the maximum-likelihood heavy-atoms parameters refinement performed using the program SHARP [4] coupled to the addition of the native data set in the phases calculation and the use of the solvent flattening program SOLOMON [2] were decisive in obtaining a clear, unambiguous electron density map into which the molecular model could be constructed readily. The atomic model, refined with the program X-PLOR [5], shows a final R-factor of 21,8 % (R_{free} = 27,9 %) between 7 and 2.2Å.

The structure of CRY is made of six α-helices and one antiparallel β sheet (Figure 2) [6]. It characterises a *new type of protein folding*. The necrogenicity-related residue 13 is located on the surface of the molecule, well exposed to the solvent on a rather peripheral site. Why this single residue has such an effect on the necrogenicity is not known. Two interesting remarks can be made. First, an original structural feature is observed, consisting of an omega loop facing the antiparallel β sheet. This part of the molecule, which has been called *beak-like motif*, corresponds to a highly conserved region of the sequence and therefore it is likely to have an important functional role. It could be the recognition site with a partner. Secondly, the side chain of Tyr87 is plunging into the hydrophobic core of the molecule. In the crystal structure of a mutant of CRY, the side chain of Tyr87 was found oriented outside of the molecule, creating a hydrophobic cavity in which the electron density of a ligand has been identified. What kind of a ligand is it ? Very little is known presently about the function of this molecule by the fungi and how the protein interacts with plants. Further functional analysis of the molecule will require more information about these key questions.

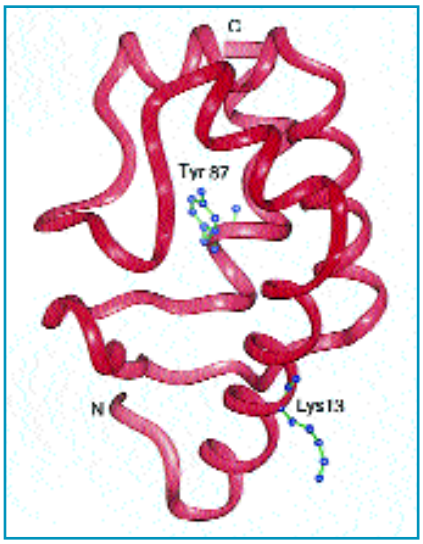

Fig. 2: Folding diagram of cryptogein showing the original beak-like motif on the left side of the structure, the hydrophobic cavity near Tyr87 and the location of the residual 13, critical for the toxicity of the molecule.

SEARCHING FOR NEW ANTIBIOTICS

Antibiotics have been in extensive clinical use over the past 50 years in antibacterial therapies, saving countless lives by killing the bacteria responsible for infectious diseases such as pneumonia, meningitis, and tuberculosis. As a result of the high efficacity of antibiotics, such as the β-lactams (penicillins and cephalosporins) and the glycopeptides (vancomycin), the general population now expects that any bacterial infection will be easily cured by one of these miracle drugs. However, the days of the miracle drugs may be coming to an end as their therapeutic value is now largely reduced or totally annihilated by the emergence and spreading of various resistance mechanisms (for reviews see Science 264: 360-393, 1994).

The existence of antibiotic-resistant strains of bacteria is nothing new, penicillin resistance strains of bacteria were observed only a few years after its clinical debut in 1942. Nonetheless, for decades the pharmaceutical industry has managed to stay ahead of the resistance by slightly modifying the structures of their antibiotics. But the modifications have continuously been proven to be only a temporary fix for the problem as the bacteria quickly adapt to the modifications. Clearly, what is needed is not a slight modification of the classical antibiotic but rather a change in the target.

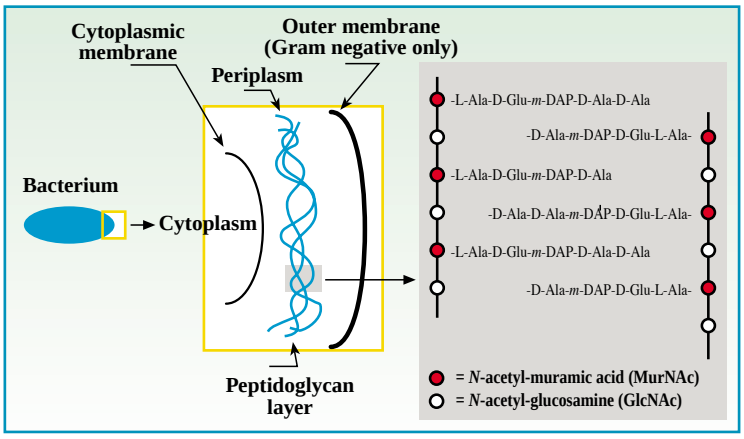

Fig. 3. Structure of the bacterial peptidoglycan layer. The bacterial cell wall is constituted by the assembly of parallel long peptidoglycan chains which are crosslinked by bonds established between the side chains, forming a huge 2-dimensional bag shaped single macromolecule. The bacteria cannot live without this cell wall. Many antibiotics act as inhibitors of the peptidoglycan synthesis.

The majority of the antibiotics in clinical use inhibit the biosynthesis of the peptidoglycan layer, a large mesh-like structure which completely surrounds the bacterial cell. The peptidoglycan (Figure 3) is formed by linear repeating disaccharide chains which are interconnected by short polypeptides which are derived from the pentapeptide unit: L-Ala-D-Glu-*m*-Dap-D-Ala-D-Ala. This assembly is essential to the survival of the bacteria in that it prevents the bacteria from bursting from the high internal osmotic pressure. The antibiotic penicillin is an inhibitor of the enzymes which cross-link the peptide chains of the peptidoglycan, one of the later steps of the peptidoglycan synthesis. The new approach, followed in the framework of the present study, is to look for inhibitors of an enzyme involved in the earlier stages of peptidoglycan biosynthesis. As such, the enzymes of the biosynthetic pathway of the UDP-*N*-acetylmuramoyl-pentapeptide, the peptidoglycan precursor, represent attractive targets for the development of new antibiotics.

In the search for new antibiotics detailed structural knowledge of the target enzyme is of primary importance. Using this knowledge, strategies can be developed for the rational design of novel inhibitors. The present structure determination concerns the enzyme uridine diphosphate N-acetylmuramoyl- L -alanine: D -glutamate ligase (MurD). The work stems from a collaboration between the Laboratoire de Biochimie Moléculaire et Cellulaire (Université de Paris-Sud, Orsay) and the Laboratoire de Cristallographie Macromoléculaire (I.B.S., Grenoble). MurD catalyses the addition of D-glutamate to the nucleotide precursor UDP-MurNAc-L-Ala forming a L-Ala-D-Glu linkage that is present in the peptidoglycan of all eubacteria. Inhibition of MurD stops the biosynthesis of the precursor and therefore interrupts the construction of the bacterial cell wall.

The structure of MurD was solved to 2.8 Å by MAD analysis of the selenomethionyl protein using data collected from a single frozen crystal on the D2AM beamline [7]. As much as 1,120 CDD images of 1242 x 1152 pixels were recorded and subsequently treated by the program XDS [1]. Approximately 61,000 reflections were collected at each of the four wavelengths (remote: 0.9827 Å, f" inflection: 0.9797 Å, f" peak: 0.9794 Å, remote: 0.9762 Å) giving values of R_{sym} between 3.6 and 4.4 %. The seleno-MurD (437 a.a., 47 kDa) was obtained by expression in Met - *E. Coli* and contained 12 Se atoms. The values of f' and f" of Se near the absorption edge were determined in the usual way by reference to the fluorescence spectrum of the protein crystal measured on the diffractometer. The Se partial structure factors, calculated using MADSYS [8], were used with the direct methods option of SHELXS-86 [9] to locate the selenium sites. Refinement of the heavy atom parameters with calculation of the phase probabilities was performed with MLPHARE [2]. The elapsed time between the crystallisation of the seleno-MurD (Feb. 96), the MAD data collection on the D2AM (late Feb. 96) and the resolution of the structure by obtaining the first interpretable electron density map (late Apr. 96) was less than three months. The calculated phases were later improved by including mercury and iodine derivative data of the seleno-MurD collected using an «in-house» X-ray source.

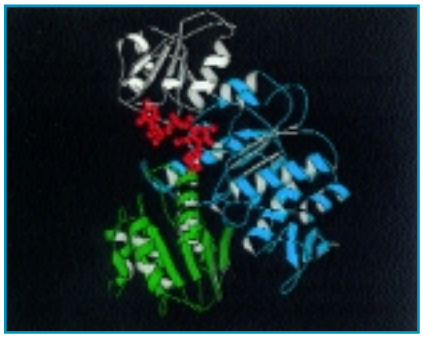

Fig. 4. Ribbon diagram of the binary complex of MurD and UMA. Domain 1 is shown in pink, domain 2 in blue, domain 3 in green and UMA in red.

The MurD structure is currently refined to 1.9 Å resolution using data collected from a crystal of the native enzyme/substrate complex on the D2AM beamline. It is the first structure reported for a member of the Mur ligase family. The structure comprises three domains of topology each reminiscent of nucleotide-binding folds: the N- and C-terminal domains are consistent with the dinucleotide-binding fold and the central domain with the mono-nucleotide-binding fold (Figure 4). The substrate UDP-N-acetylmuramoyl-L-alanine (UMA) is bound in the cleft formed between the N-terminal and central domains. Structural analysis supports a mechanism which proceeds by phosphorylation of the C-terminal carboxylate of UMA by the γ-phosphate of ATP to form an acyl phosphate intermediate, followed by nucleophilic attack by the amide group of D-glutamate to produce UDP-N-acetylmuramoyl-L-alanine-D-glutamate, ADP, and inorganic phosphate. ■

References

[1] *W. Kabsch (1988) J. Appl. Cryst., 21, 916-924.*
[2] *Collaborative Computational Project No. 4. (1994) Acta Cryst., D50, 760-763.*
[3] *T.C. Terwilliger (1994) Acta Cryst. D50, 17-23.*
[4] *E. de La Fortelle and G. Bricogne (1996) Methods in Enzymology (Carter, C.W. & Sweet R.M., eds), 472-494.*
[5] *A.T. Brünger, J. Kuryian and M. Karplus, (1987) Science, 235, 458-460.*
[6] *G. Boissy, E. de La Fortelle, R. Kahn, J.-C. Huet, G. Bricogne, J.-C. Pernollet. and S. Brunie (1996) Structure 4, 1429-1439.*
[7] *J.A. Bertrand, G. Auger, E. Fanchon, L.Martin, D. Blanot, J. van Heijenoort and O. Dideberg (1997) submitted to EMBO J.*
[8] *W.A. Hendrickson, J.L. Smith, R.P. Phizackerley and E.A. Merritt (1988) Proteins: Struct. Funct. Genet., 4, 77-88.*
[9] *G.M. Sheldrick (1990) Acta Cryst., A46, 467-473.*

From left to right, back row: K. Brown, S. Labouré, L. Claustre, R. Pinck. Back row: G. Leonard, V. Biou, F. Lapeyre, A. Thompson, V. Stojanoff, M. Mattenet, F. Felisaz.

GOING MAD ON BM14

V. BIOU[1], G. LEONARD[2], V. STOJANOFF[2], S. LABOURÉ[2], M. MATTENET[2], J. HELLIWELL[3], F. FELIZAZ[4], L. CLAUSTRE[4], F. LAPEYRE[4], K. BROWN[4] AND A. THOMPSON[4]

1 IBS AND ESRF, GRENOBLE (FRANCE)
2 ESRF, EXPERIMENTS DIVISION
3 UNIVERSITY OF MANCHESTER (UK)
4 EMBL, GRENOBLE OUTSTATION (FRANCE)

BM14 supplies a narrow bandpass, rapidly tunable source of intense X-rays for structure determination using Multi-Wavelength Anomalous Diffraction (MAD) from macromolecular crystals, and was built as a collaboration between the EMBL and the ESRF.

The MAD method has been extensively developed by Hendrickson, and his excellent review [1] gives an overview of the field as it was in 1991. For a more recent review, see Fourme et al [2].

Over the last 18 months on the beamline a number of new structures have been solved either using «pure» MAD phasing, or by incorporating phase information from elsewhere. These have, in the main, been solved using a MAR research image plate detector, which produces excellent quality data but has a readout time which is slow compared to the sample exposure times used on the beamline. To alleviate this problem, work has progressed towards the calibration [3] and usage of an Image Intensified CCD detector (II/CCD) developed at the ESRF by J.-P. Moy of the detector group [4], and resulted in several successful data collections with the detector, and the solution of a new structure by MAD phasing using the detector.

The French Collaborating Research Group beamline (D2AM) has also successfully used MAD to solve new protein structures.

BM14 has been operational since September 1995.

The bandpass with the replacement monochromator crystal currently available is approximately 2.5 x 10^{-4} from a Si(111) monochromator. A Si(311) monochromator and a second Si(111) monochromator with an improved surface finish are available for testing early in 1997. Wavelength is rapidly tunable between limits of 0.6 Å and 1.8 Å - the wavelength can be accurately and reproducibly changed within these limits within a few minutes.

MAD, AND HOW TO DO IT

One of the major barriers to resolving a macromolecular crystal structure is the solution of the phase problem, i.e. the reconstruction of the phase of the diffracted X-rays. The most common method of doing this is by using Multiple Isomorphous Replacement (MIR), i.e. by producing «heavy atom derivatives» of the crystal which are «isomorphous» or identical in terms of the arrangement of molecules inside the crystal. More recently the MAD method (Hendrickson [1]) has become increasingly popular in deriving phases, and offers significant advantages over other methods.

The great advantage of the MAD method is that it does not depend on crystal isomorphism. «Isomorphous» derivatives are rarely completely so, and tend to look worse when the crystal structure is examined in higher detail (ie at higher resolution). In principle, MAD can therefore provide better measurements of phase to higher resolution (if the crystals diffract sufficiently well). In addition, the anomalous signal depends to a lesser extent on diffraction angle than the normal scattering, so that it should (in theory at least) become more significant at higher resolution.

Table 1: Likely «heavy atom» targets for MAD measurements. Most elements with Z > 24 are suitable if they contribute sufficient anomalous signal (see Equation).

Category	*Anemalous scatterer*
Metalloproteins	
Transition metals	*Fe, Cu, Zu, Mn*
Other metals	*Ca, Mo*
Metal replacements	
Lanthanides for Ca^{2+}, Mg^{2+}	*Tb, Ho, Yb*
Mercury for Zn	*Hg*
Heavy atom complexes	
Common protein derivatives	*Pt, Au, Hg, Pb, W, U*
Cluster compounds	*Ta, W*
Building - unit analogs	
Selenomethionine or selenocysteine	*Se*
Telluromethionine	*Te*
Brominated or iodinated nucleotides	*Br, I*

Briefly, protein crystals can naturally contain or have incorporated within them «heavy atom» scatterers (see Table 1, based on Hendrickson [1]) which exhibit anomalous scattering in the X-ray region (the bulk of the atoms making up a large protein structure being carbons, nitrogens and oxygens, which exhibit no anomalous scattering in the X-ray region). Heavy atom incorporation is discussed in Pappa et al [4].

If the energy of the incident X-ray beam is close to the energy of an electron transition from an inner bound state to a higher state or the continuum of states, there results both an absorption of the incident X-rays and a resonance in sympathy with the natural frequency of the bound electron, which peaks when the incident X-ray energy is identical to the energy required for the (quantum mechanically allowed) transition. This in turn modifies the overall contribution of the «heavy atom» to each diffraction spot, and gives rise to «anomalous» differences between intensities of mirror plane related reflections (Bijvoet pairs) recorded at any one wavelength, and «dispersive differences» between the same reflection measured at different wavelengths. The information from the anomalous differences can be used to locate the «heavy atom» in the unit cell, and the combined information from the anomalous and dispersive differences can be used to calculate a unique phase for each reflection and hence «solve» the crystal structure.

A MAD experiment therefore consists of measuring the absorption (or more frequently, fluorescence) spectrum of the «heavy atom» as a function of incident X-ray energy, and collecting several X-ray diffraction data sets at energies chosen to maximise both the anomalous and dispersive signals. Figure 1 shows a typical fluorescence spectrum from a protein crystal (in this case a class II aldolase, modified to contain Se instead of S in methionine residues, Hunter [6]).

Fig. 1: Typical fluorescence spectrum from a Se-met protein crystal.

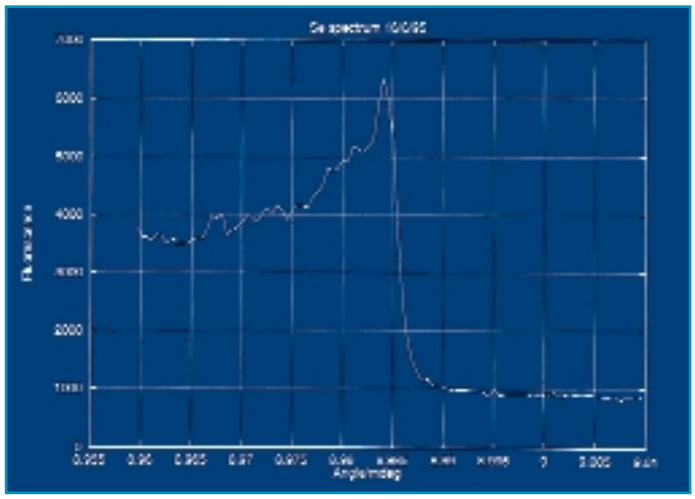

Unfortunately the size of these signals is small, often only a few percent, and is given by (Smith [7]) :-

$$\Delta_{anom} = \sqrt{\frac{N_{anom}}{2}}\,\frac{2f''_{anom}}{\langle |F_p| \rangle}$$

$$\Delta_{disp} = \sqrt{\frac{N_{anom}}{2}}\,\frac{|f'_{\lambda_1} - f'_{\lambda_2}|}{\langle |F_p| \rangle}$$

where $\langle |F_p| \rangle$ is the total scattering due to the molecule, f_{max}'' is the maximum «anomalous» scattering component arising from the absorption of X-rays, f'_{λ_i} is the «dispersive» or resonant component at wavelength «i», N_{anom} is the number of anomalous scatterers per molecule, and Δ_{anom} and Δ_{disp} refer to the maximum anomalous and dispersive intensity differences expected as a fraction of the overall scattering. Note that these expressions only apply when there is a single species of anomalous scatterer present, and the anomalous scattering is a small fraction of the overall scattering. For those wishing to make these calculations to test the feasibility of their own MAD experiment, values of f' and f'' can be found in (for example) Sasaki [8]. The behaviour of these quantities around an X-ray absorption edge are indicated in Figure 2, which also shows how «normal» and «anomalous» scattering adds to give the overall «observable» structure factor.

Fig. 2: a) A theoretical Se absorption spectrum. The f' value is always negative in the diagram, and reaches a minimum at the absorption edge. b) An Argand diagram showing how F_{obs}, the «observable» structure factor is made up of the scattering due to the anomalous scatterer F_A, F_A' and F_A''. F_P is the scattering due to the rest of the atoms in the protein.

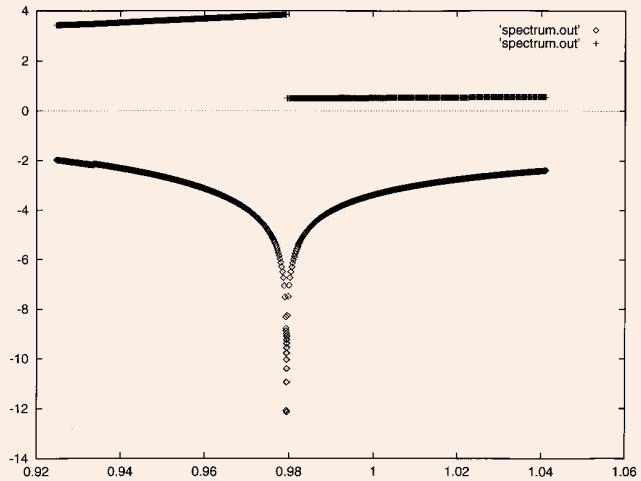

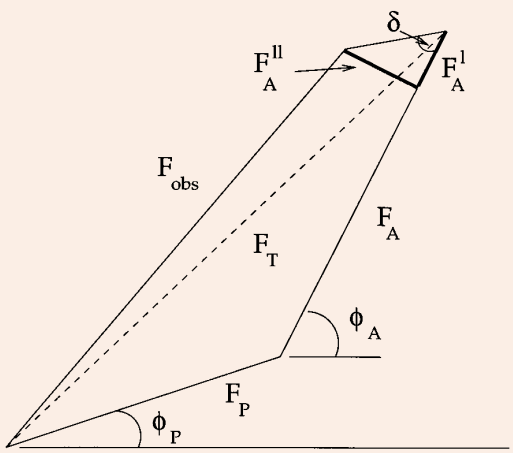

Table 2 gives values of the expected maximum anomalous and dispersive differences for a «typical» case of a 30 kDa molecule with various anomalous scatterers. Since these signals are small (often comparable with the intrinsic accuracy of diffraction data), care has to be taken in their measurement.

In particular :

• If Bijvoet related reflections are measured close together in time (ideally on the same image) systematic errors due to variation of the intensity of the incident X-ray beam, variation of the exposure time due to a faulty X-ray shutter, sample radiation damage, etc. are eliminated hence giving an accurate measurement of the anomalous differences. This requires alignment or «setting» of the crystal in a particular orientation, and is not always possible due to the morphology of the sample or a limitation in the beamline goniometer. In this latter case, data can be collected in «inverse beam geometry» or by rotating the crystal to view the Bragg planes in the opposite sense and hence record Bijvoet mates in successive images (but still close together in time).

The stability of modern synchrotron sources such as the ESRF, and the cryo - protection of samples which greatly slows down radiation damage, considerably reduces systematic errors in the data so that very accurate alignment of the sample is not always necessary (a great simplification of data collection procedures).

• Since the signal is small, care must be taken to minimise measurement noise (X-ray background, electronic noise from area detectors) and counting time must be increased to give a signal with sufficient statistical accuracy to discriminate between the normal and anomalous scattering. In the case of weak, high resolution diffraction spots, this often entails collecting data twice at different X-ray exposures, or by «extending» the detector dynamic range by using absorbers to weaken the low resolution diffraction pattern (or buying a higher dynamic range detector!)

• The structure is calculated from a knowledge of the intensity and phase of all reflections. Therefore care must be taken not only to measure «complete» data, but also to measure all Bijvoet pairs. This can be easily achieved by the use of a suitable prediction program, such as the STRATEGY option of MOSFLM (Leslie). It is wise to have sufficient redundancy in the data to be able to distinguish between good measurements of intensity and those subject to error due to being close to spurious detector «events» (ice rings, zingers, dirty thumb prints etc).

Anomalous scatterer	*NO of scatterers*	*Percentage anomalous difference*
Pt	*1*	*4.7*
Se	*1*	*1.8*
Se	*4*	*3.5*
Hg	*1*	*4.3*
Yb	*1*	*4.9*

Table 2: Theoretical maximum anomalous signals at the peak of the absorption edge. Note that scatterers that exhibit a «white line» (for example Se in Se-met) have an amplified anomalous effect. Signals below 3 % are very hard to measure unless X-ray data is of excellent quality.

A RECENT MAD STRUCTURE

The structure of Maclura Pommifera Agglutinin (a moraceae plant lectin) is of great medical interest due to its high affinity and specificity to bind tumour specific molecules, antigens, on the surface of carcinoma cells (Table 3) from which 85% of cancers develop. This structure was solved in collaboration with a group from the Department of Cancer Biology (Cleveland Cancer Research Clinic) protein crystallography laboratory headed by Dr X. Lee, and was the first MAD structure to be solved on BM14 using the II/CCD detector.

Details of the crystal and molecule are given in Table 4. Although the protein is itself rather small (153 or 154 amino acid residues), structure solution was not easy due to the great difficulty in finding isomorphous derivative crystals. A possible Pb containing crystal was found to give a strong fluorescent spectrum on the beamline. Hence three datasets were collected spanning the lead absorption edge. Figure 3 shows the anomalous and dispersive Pattersons from data collected close to the absorption edge, demonstrating quite clearly the high data quality and stability of the II/CCD detector. MAD phasing proceeded by finding the Pb atoms by solving the Patterson map (two high-occupancy sites

Intradermal delayed-type hypersensitivity response to erythrocyte-derived T-antigen (DTHR-T), at initial visit, of carcinoma patients and controls.

Category	*DTHR-T+/total tested*
Lung	
Carcinoma	
Adeno	*45/49*
Brochioloalveolar	*5/6*
Small-cell	*15/17*
Squamous-cell	*12/14*
Large-cell anaplastic	*1/1*
Other pleuropulmonary cancers	*1/5*
Benign diseases	*2/35*
Pancreas	
Adenocarcinoma	*23/26*
Pancreatitis	*0/13*
Breast adenocarcinoma	
Ductal	
Stage I noninfiltrating	*10/12*
Stage I infiltrating	*32/37*
Stage II and III	*37/42*
Stage IV	*17/17*
Total	*96/108*

Table 3: Specificity of MPA to T-Antigen binding.

Table 4: Crystal parameters for MPA.

MPA & p-hydroxymercuriphenyl sulfonic acid
Space group: C222.
Cell parameters: a = 58.97 Å, b = 119.5 Å and c = 155.41 Å
Two molecules of (a + b) per asymmetric unit.
Crystallization conditions: hanging drop method.
Reservoir solution: 0.5 M Li_2SO_4 and 7.5 %. PEG 8000 plus 1 % octyl-β-D-glucopyranoside (O.G.).

easily identified), and scaling and phasing the data using programs in the CCP4 [9] program suite (SCALEIT and MLPHARE). The phasing statistics were «encouraging», the overall figure of merit being 69% to 2.9Å resolution, and the map quality excellent. The high quality of the map was perhaps unsurprising given the modest size of the protein and the large anomalous signal from the two Pb atoms. The protein was traced using a solvent flattened map (DM, cowtan). The model was then used to find a molecular replacement solution for data collected from crystals with the tumour antigen Galβ,3GalNAc bound (data to 2.2 Å resolution collected at the Cleveland Cancer Research Clinic using a rotating anode). The current refined model, showing the antigen bound, is shown in Figure 4.

MAD maps can often be of high quality if the data collected is complete, even for cases where the anomalous signal is «more typical» i.e. lower! The protein ALA dehydratase, studied for the last 6 years by Dr J. Cooper of Birkbeck College, London, is extremely difficult to derivatise, and certain metals (for example Pb) inhibit the protein. The protein itself, however, contains five methionine residues in a 38 kDa molecular weight, so biological substitution of selenium for sulphur provided an alternative approach to obtaining phase information (as suggested by Hendrickson [10]). A MAD experiment was performed using the selenated form of the protein, yielding an extremely good electron density map which was phase extended to 2.5 Å resolution. The data were collected from a randomly oriented crystal using a MAR image plate (loaned from the EMBL), and phases calculated using MLPHARE [9]. The overall figure of merit was 62%, with an overall phasing power of 1.3 and Cullis factor of 0.69 (to 3.5 Å). Figure 5 shows a section of alpha helix from the solvent flattened map, illustrating the extremely high quality of the electron density map.

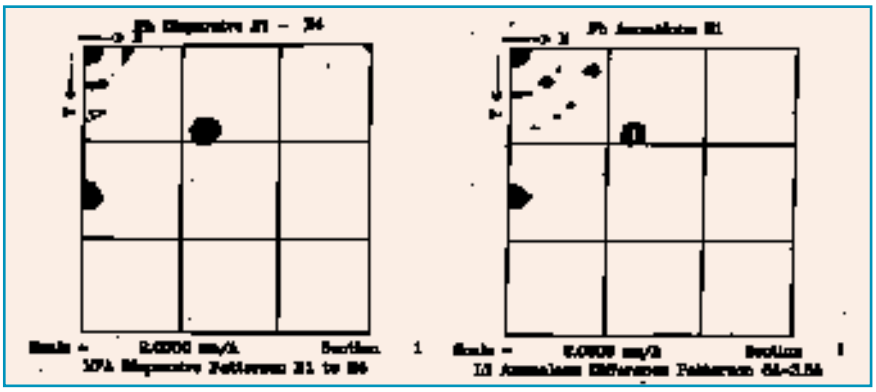

Fig. 3: Zeroeth «w» sections of the anomalous and dispersive Pattersons, contoured in 0.5 sigma intervals with a cutoff of 2 sigma.

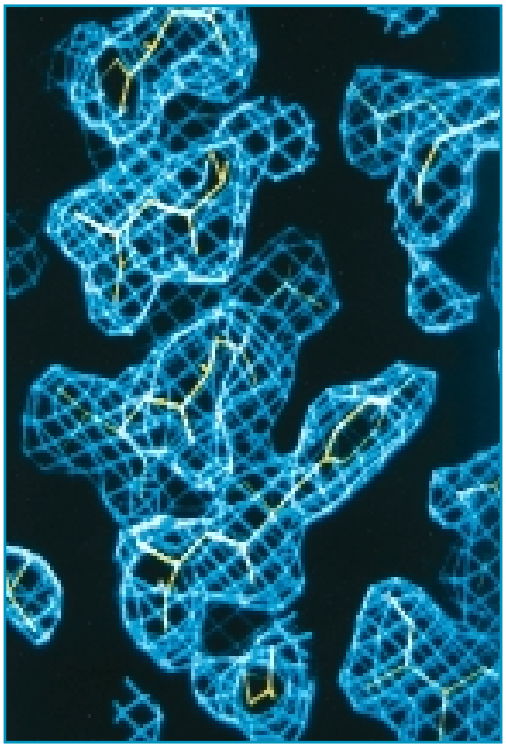

Fig. 5: A portion of a-helix form the «MAD» electron density map of ALAD (courtesy of J. Cooper).

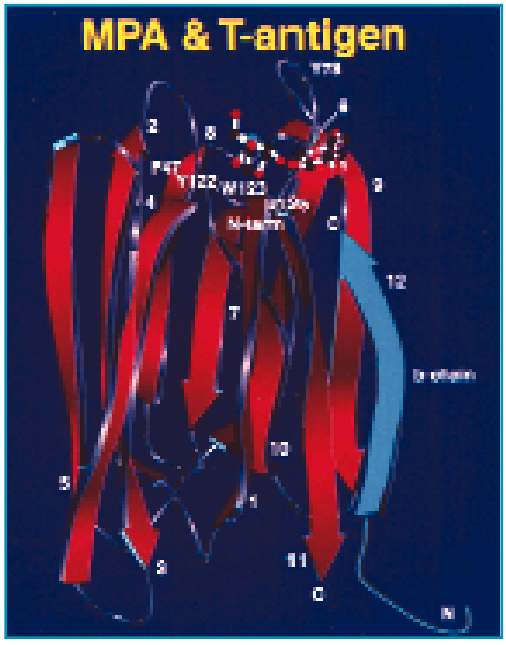

Fig. 4: Current model of MPA with T-antigen bond.

SOME TECHNICAL DEVELOPMENTS

Significant technical progress has also been made on the beamline, with the first experiments being performed with the rapid image plate changer – a device capable of changing an exposed plate in 0.15 s. Figure 6 shows a plate being mounted on the new system. The image plates themselves are identified by a bar code reader both as they are exposed in the X-ray beam and just before reading in the FUJI BAS2000 image plate scanner. Details of the oscillation angle of the exposure, wavelength, time of exposure, etc. are recorded in a data base which can be displayed using a network browser. The knowledge of the time elapsed between exposure and reading of the plate permits a correction to be made for the decay of the photo stimulated luminescence. A test experiment was performed using this

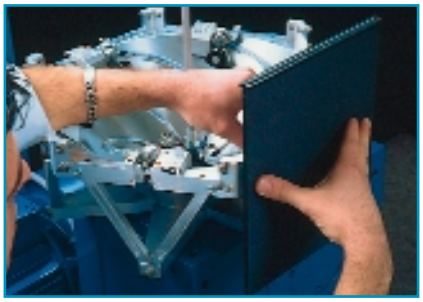

Fig. 6: Mounting an image plate on the rapid plate changer.

detector and crystals of ribonucleotide reductase (RNR, a known structure studied in the laboratory of P. Nordlund at the University of Stockholm). RNR will not crystallise in the absence of Hg, and can contain up to 10 Hg binding sites in a protein of 530 amino acids. Hence the anomalous signal is potentially very large and a MAD experiment feasible. The crystals diffract to high resolution. Three wavelengths of data were collected around the Hg absorption edge and inspection of

Dataset	Site n°	Occupancy	
		Dispersive	Anomalous
L1	1	8.266	10.112
	2	8.521	8.745
	3	7.987	9.830
	4	6.943	8.828
	5	3.502	3.821
	6	3.158	3.628
	7	1.972	2.206
L3	1	2.639	10.328
	2	1.743	8.553
	3	2.813	10.141
	4	2.823	9.052
	5	0.606	3.652
	6	0.654	3.411
	7	0.375	0.040
L2	1	0.000	7.123
	2	0.000	5.902
	3	0.000	6.748
	4	0.000	6.327
	5	0.000	2.527
	6	0.000	2.460
	7	0.000	1.363

Table 5: Site occupancies after refinement.

the Patterson map calculated at the peak of the Hg absorption edge yielded seven sites of varying occupancy.

Table 5 shows the occupancy of the various Hg sites (refined from the program MLPHARE [9]. These sites were used to calculate phases to high (2.0 Å) resolution, a typical section of electron density being shown in Figure 7. The impact of collecting MAD data to high resolution is discussed in Reed [11].

Other new technical developments on the beamline include the new crystal mounting laboratory and data processing room adjoining the beamline, a joystick for quick and easy sample alignment, and improved cryogenic facilities for freezing, storing and transferring crystals to the X-ray beam.

The program MADNES [12] for collecting and analysing data collected with a diffractometer and area detector, has been modified in order to collect data using the beamline goniostat and the II/CCD detector. A graphical user interface PXGEN (Kinder [13]) developed at the PPSRC Daresbury Laboratory, UK, allows easy control of data collection, and has recently been installed for testing on the beamline.

WORKING WITH MAD

In order to further promote the MAD technique, a study week was arranged in Grenoble in June 1996 to discuss and teach the method to scientists from Europe, the USA and Japan. Demand for places exceeded availability by a ratio 3:1, so that many good applicants had to be rejected. Hence a second MAD Practical Course will be held in Grenoble in June 1997, this time with funding from the European Molecular Biology Organisation.

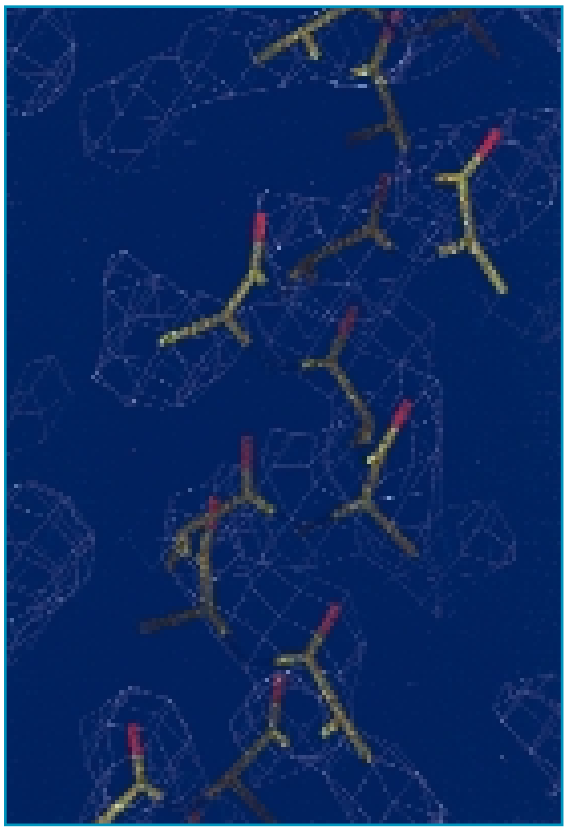

Fig. 7: Section of the electron density map of RNR showing one of the two Fe sites (courtesy of P. Nordlund).

CONCLUSION

MAD phasing is now an extremely important tool with which X-ray crystallographers can solve the «phase problem» to reveal the internal folding of protein structures of great biological interest. The additional intensity and stability of the ESRF beam provides an excellent facility for the exploitation of this technique in Europe. This improvement will be further consolidated when an undulator beamline for MAD protein crystallography (Shapiro et al [14], Biou et al [15]) becomes available at the ESRF in 1999, which should give a tenfold intensity gain enabling more and more complicated structures to be solved using the MAD method. ■

References

[1] W. A. Hendrickson, Science 254 (1991) pp 51 - 58.

[2] R. Fourme, W. Shepard and R. Kahn, Progress in Biophysics and Molecular Biology 64 (1996) pp 167 - 199.

[3] A. P. Hammersley, S. O Svensson, J-P. Moy, A. Gonzalez, K. Brown, W. Burmeister, S. McSweeney, A. Thompson,. accepted for publication in Journal of Synchrotron Radiation (1997).

[4] J-P Mo,. Nuclear Instruments and Methods A 346 (1994) pp 641 - 644.

[5] H. S. Pappa, A. E. Stewart and N. Q. McDonald, Current Opinion in Structural Biology 6 (1996) 611 - 616.

[6] S. J. Cooper, G. A. Leonard, S.M. Mc Sweeney, A.W. Thompson, J.H. Naismith, S. Qamar, A. Plater, A. Berry and W. N. Hunter., Structure 4 (1996) pp 1303 - 1315.

[7] J. L. Smith, Current Opinion in Structural Biology 1 (1991) pp 1002 - 1011.

[8] S. Sasaki, KEK Report 88-14 (1989), National Laboratory for High Energy Physics, Tsukuba, Japan.

[9] CCP4, Acta Crystallographica D (1994) pp 760 - 763.

[10] W. A. Hendrickson, Transactions of the American Crystallographic Association 21 (1985)pp 11 - 21

[11] R. J. Reed, Structure 4 (1996) pp 11 - 14.

[12] A. Messerschmidt and J. W. Pflugrat, Journal of Applied Crystallography 20 (1987) pp 306 - 315.

[13] S. H Kinder, S. M. McSweeney and E. M. H. Duke, Journal of Synchrotron Radiation 3 (1996) pp 296 - 300.

[14] L. Shapiro, A. M. Fannon, P. D. Kwong, A. Thompson, M. S. Lehmann, G. Grübel, J.-F. Legrand, J. Als-Nielsen, D.R. Colman and W. A. Hendrickson, Nature 374 (1995) pp 327 - 337.

[15] V. Biou, A. Gonzalez, J. R. Helliwell, S. McSweeney, J. L. Smith and A.Thompson, Report to the ESRF Science Advisory Committee (1995).

Assessment of Bone Micro-architecture using 3D Computed Microtomography

M. Salomé[1,2], F. Peyrin[1,2], P. Cloetens[2,3], J. Baruchel[2], P. Spanne[2], P. Suortti[2] and A.M. Laval-Jeantet[1]

1 Creatis, INSA, Lyon (France)
2 ESRF, Experiments Division
3 EMAT, RUCA, Antwerp (Belgium)

From left to right: M. Salomé, J. Baruchel, F. Peyrin and P. Spanne.

The investigation of trabecular bone structure requires a high spatial resolution imaging tool, providing non-destructively 3D images of bone samples. Synchrotron X-ray computed microtomography (CMT) fulfils these requirements and is used to study the evolution of bone structure with aging.

Most bones are composed of a cortical shell of compact bone surrounding an internal part of trabecular bone made of small rods and plates called trabeculae. The proportion of trabecular bone is particularly high in the vertebra, the iliac crest and the os calcis. The importance of the organisation of trabeculae with respect to the fracture risk has been highlighted by different authors. Indeed, the mechanical properties of trabecular bone depend both on the mineral density and on the microarchitecture. Bone mineral density is often estimated *in vivo* using Dual Energy X-ray Absorptiometry (DEXA), which is based on measurements at two different energies and gives an average value of the mineral content of bone (hydroxyapatite). The quantification of bone microarchitecture is mainly based on histology. Histological techniques consist in cutting bone biopsies, generally taken from the iliac crest, in very thin slices which are then imaged by X-ray microradiography or stained and observed using an optical microscope. Image processing techniques are then applied to extract histomorphometric parameters quantifying bone structure in terms of shape and connectivity [1-2]. This technique is destructive and two-dimensional, and only gives an estimate of the properties of the three-dimensional (3D) structure of bone. Moreover, it has been shown that the structure of bone is anisotropic, and requires 3D studies with high spatial resolution since the mean size of the trabeculae is around 100 microns [3]. Non-destructive imaging like X-ray computed tomography (CT) [4-8], or Magnetic Resonance Imaging (MRI) [9] has been developed to fulfil these requirements. X-ray computed tomography and microtomography (CMT) only differ because they have different spatial resolutions. X-ray absorption computed tomography is widely used for medical imaging (scanners), and is performed by reconstructing a 2D or 3D image of a patient from attenuation measurements at different angular positions. The CMT technique is greatly improved by the use of synchrotron radiation. Unlike laboratory X-ray sources, synchrotron radiation offers the possibility to select X-rays with a small energy bandwidth from the wide and continuous energy spectrum, while at the same time keeping the photon fluence rate high enough for efficient imaging. This possibility is of great interest for microtomography since it allows high spatial resolution images to be generated and avoids beam hardening artefacts, which occur with the use of polyenergetic beams for tomographic imaging. Synchrotron X-ray computed microtomography, which provides high resolution 3D images, is well suited for studying porous media in general, [11] and trabecular bone in particular.

Bone is a living tissue under continuous remodelling since the structure is resorbed by cells called osteoclasts and reconstructed by osteoblasts. If the balance between osteoclast and osteoblast activities is disturbed because of a pathology or aging, the architecture of bone deteriorates. Not only the quantity of bone mineral decreases, but bone architecture also becomes weaker due to the structural changes, which may lead to severe vertebral or hip fractures. We are particularly interested in studying the evolution of bone structure with

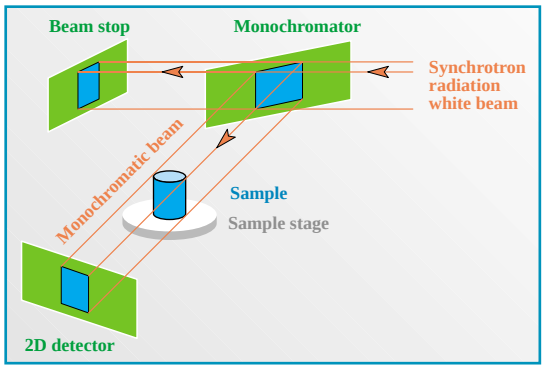

Fig. 1: Scheme of the acquisition set-up.

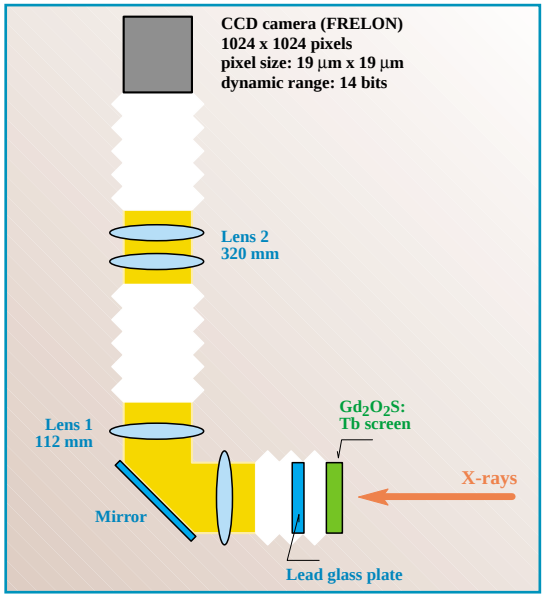

Fig. 2: CCD based 2D detector.

aging. The purpose of this work is to improve the understanding of the changes occurring in bone architecture by finding relevant parameters characterising bone structure and studying their correlation with age.

METHODS

In conventional CT scanners, the sample is usually fixed while the X-ray source and the detector rotate around it. This geometry is of course not possible with a synchrotron radiation source, and the rotation must be applied to the sample. Therefore, the sample to be imaged is mounted on a translation/rotation stage allowing precise alignment in the beam. A 2D detector records projections of the sample for different angular positions as shown in Figure 1. A typical scan includes 900 projections of the sample over 180 degrees. The detector is the most critical part of the set-up since it determines the spatial resolution in the image, contrary to first generation tomography, where the spatial resolution depends on the beam size or the sampling distance. The detector we used is based on the FRELON CCD (Charge Coupled Device) camera developed by the ESRF Detector Group [10]. It consists of a 2D CCD array with 1024 x 1024 elements, each 19 x 19 μm^2 and offers a dynamic range of 14 bits. A thin scintillating Gd2O2S:Tb layer deposited on glass converts X-rays to visible light. Light optics then magnify the image of the screen and project it onto the CCD. The CCD camera is mounted perpendicularly to the X-ray beam in order to protect it and avoid direct interactions which cause noise in the recorded images. Different lenses and scintillators with different thicknesses can be used to adjust the pixel size to the sample size. For bone structure studies, we used an optical magnification of 2.86 resulting in a pixel size of 6.65 microns and a field of view of 6.8 mm x 6.8 mm. A schematic drawing of the detector is presented in Figure 2.

A 3D filtered back projection algorithm, implemented in C language, is used to reconstruct a 3D image of the sample from the series of 2D projections. Given the large quantity of data to be handled (about 2 Gigabytes per sample), the reconstruction process is quite time-consuming. Therefore the reconstruction program was parallelised on the ESRF Networked Interactive Computing Environment (NICE) using PVM (Parallel Virtual Machine), leading to considerable time saving (4 hours on 9 workstations instead of several days on a single workstation to reconstruct a $(512)^3$ volume).

RESULTS

A CMT experiment was performed on the Topography and High Resolution Diffraction beamline (ID19). A series of ten bone samples (4 mm x 4 mm x 4 mm) cut from human vertebrae embedded in lucite were imaged using 20 keV X-rays. The images presented in Figures 3 to 5 show volume rendering views of samples from women at three different ages. Ray tracing was used to obtain these views. The structural change (bone loss, decrease in connectivity) with age is obvious.

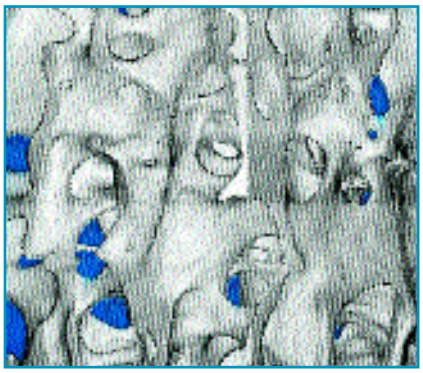

Fig. 3: 3D tomographic reconstruction of a vertebra sample from a 33 year old woman. The field of view is 4 mm x 4 mm.

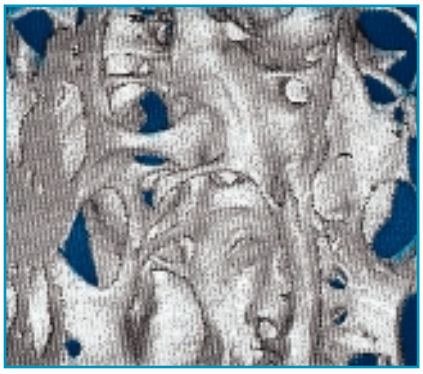

Fig. 4: Same as Figure 3, 55 year old woman.

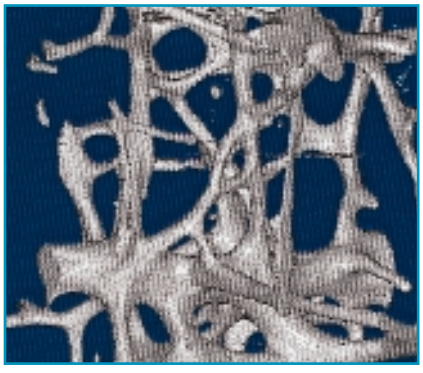

Fig. 5: Same as Figure 3, 72 year old woman.

The first step in the analysis of images is to distinguish bone tissue from the background, here lucite. This operation is called segmentation and provides a binary image. The contrast in the images was high enough to make possible segmentation with a global threshold, equal for all images. Conventional parameters defined in histomorphometry such as trabecular bone volume fraction in the sample (denoted BV/TV), trabecular bone surface-to-volume ratio (BS/BV), and mean trabecular thickness (Tb.Th), were extracted from the binary images and correlated to age. As an example, the age dependency of BV/TV is presented in Figure 6. A significant correlation coefficient (r = 0.75) was found between BV/TV and age.

The measured parameters were compared to histomorphometric measurements performed previously on a histological slice of the same vertebra and were found to be in good agreement. A correlation with r = 0.8 was also established between BV/TV and the ash weight measurement performed on a 1 cm^3 sample of the same vertebra (see Figure 7). Synchrotron radiation microtomo-graphy confirms the results obtained in histology, and overcomes its limits. Firstly the measurements performed using microtomography should be more accurate because they are done on a larger sample than a single isolated slice and thus take into account the variability inside the vertebra, and secondly this technique allows 3D connectivity measurements which can hardly be estimated from 2D slices and justify fully the need for 3D images of trabecular bone. We are currently working on developing such 3D connectivity parameters derived from so called skeletonisation of the 3D images [11].

CONCLUSION

Synchrotron radiation microtomo-graphy is an excellent tool for investigations of trabecular bone because it gives access to the 3D organisation of bone structure at a relevant scale. So far, we have studied alterations of bone structure as a function of age in women, but many other studies are possible in the field of bone research, e.g. the effect of drugs against bone diseases like osteoporosis and foetal vertebrae growth. ■

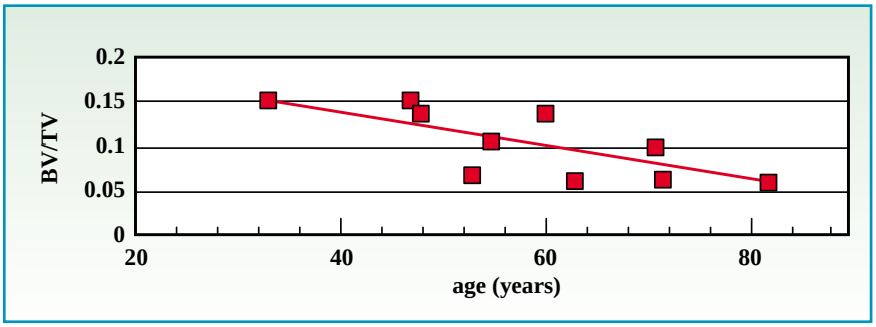

Fig. 6: BV/TV plotted as a function of age.

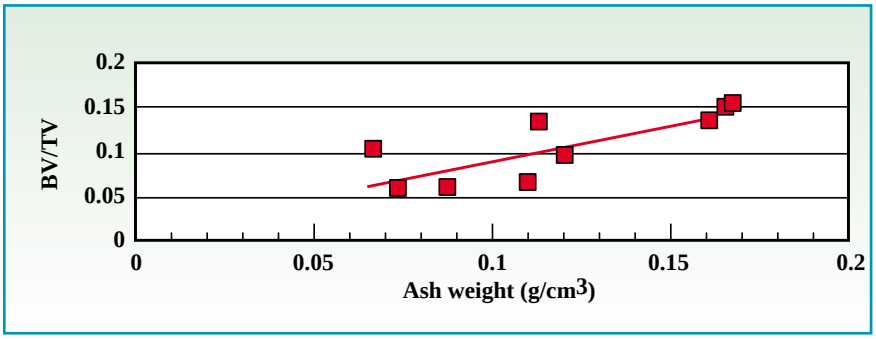

Fig. 7: BV/TV plotted as a function of ash weight measured on a 1 cm^3 sample.

References

[1] A.M Parfitt, C.H.E. Mathews, A.R. Villanueva, M. Kleerekoper, B. Frame, D.S. Rao, «Relationships between surface, volume, and thickness of iliac trabecular bone in aging and in osteoporosis», Journal of Clinical Investigation, vol 72, p 1396-1409, 1989.

[2] L.A Feldkamp, S.A Goldstein, A.M. Parfitt, G. Jesion, M. Kleerekoper, «The direct examination of three-dimensional bone architecture in vitro by computed tomography», Journal of Bone and Mineral Research, vol 4 p 3-11, 1989.

[3] C. Bergot, A.M. Laval-Jeantet, F. Preteux, A. Meunier, «Measurement of anisotropic vertebral trabecular bone loss during aging by quantitative image analysis», Calcified Tissue International, vol. 43 p 143-149, 1988.

[4] P. Rüegsegger, B. Koller, R. Müller, «A microtomographic system for the non-destructive evaluation of bone architecture», Calcif. Tiss. Int., vol 58, p 24-29, 1996.

[5] F. Peyrin, J.P. Houssard, E. Maurincomme, G. Peix, R. Goutte, A.M. Laval-Jeantet, M. Amiel, «3D display of high resolution vertebral structure images», Computerized Medical Imaging and Graphics, vol 17, p 251-256, 1993.

[6] U. Bonse, F. Busch, O. Gunnewig, F. Beckmann, R. Pahl, G. Delling, M. Hahn, W. Graeff, «3D computed X-ray tomography of human cancellous bone at 8 mm spatial and 10E-4 energy resolution», Bone and Mineral, vol 25, p 25-38, 1994.

[7] M. Pateyron, F. Peyrin, A.M. Laval-Jeantet, P. Spanne, P. Cloetens, G. Peix, «3D microtomography of cancellous bone samples using synchrotron radiation», SPIE Medical Imaging 96, Physics of Medical Imaging, proc. vol 2708, p 417-426, February 1996.

[8] K. W. Jones, B.M. Gordon, G. Schidlovsky, P. Spanne, X. Dejun, R.S. Bockman and A.J. Saubermann, «Biomedical elemental analysis and imaging using synchrotron X-ray microscopy», 1990

[9] S. Majumdar, D. Newitt, M. Jergas, A. Gies, E. Chiu, D. Osman, J. Keltner, J. Keyak, Genant, «Evaluation of technical factors affecting the quantification of trabecular bone structure using magnetic resonance imaging», Bone, vol 17, n° 4, p 417-430, 1995.

[10] J. C. Labiche, J. Segura-Puchades, D. Van Brussel, J. P. Moy, «FRELON camera: Fast REadout LOw Noise», ESRF Newsletter, n° 25, p 41-43, March 1996.

[11] W. B. Lindquist, S. M. Lee, D. A. Coker K.W. Jones, P. Spanne, «Medial axis analysis of void structure in three-dimensional tomographic images of porous media», Journal of Geophysical Research, vol 101, n° B4, p 8297-8310, April 1996.

ACKNOWLEDGEMENTS

We thank the members of the Topography Group for help during data acquisition and the ESRF Detector and Programming Groups for their assistance with the detector. Thanks also to Ulrich Mayerhofer from the Computing Services for parallelising the 3D reconstruction program and to Catherine Bergot, Laboratoire de Radiologie Expérimentale (Paris VII, France), for providing the histological measurements on the bone samples.

From left to right, back row: T. Tomizaki, J.-C. Castagna, F. Cipriani, H. Blampey, W. Burmeister, S. Wakatsuki. Front row: L. Claustre and C. Wilkinson.

A Large X-ray Image Plate Scanner for a Weissenberg Camera on ID14

F. Cipriani[1], J.-C. Castagna[1], L. Claustre[1], H. Blampey[1], C. Wilkinson[1], T. Tomizaki[2], W. P. Burmeister[2] and S. Wakatsuki[2]

1 EMBL, Grenoble (France)
2 ESRF, Experiments Division

As a result of the high brilliance of X-ray beams from undulators on third generation synchrotron sources, it is now possible to collect X-ray diffraction data from small crystals of membrane proteins and large bio-molecular assemblies such as viruses and ribosomes. In these applications, a large active area of the detector and the high duty cycle of the data acquisition are important factors for efficient data collection. A new system has been designed and is now under development as a collaboration between the EMBL and the ESRF.

We have designed a data acquisition system for one of the experimental stations, EH3, of Protein Crystallography beamline ID14 with a combination of (1) a 2k by 2k CCD detector for fast screening of crystals and determination of the orientation matrix, and (2) a Weissenberg camera with a very large active area using image plates, an industrial robot for automatic exchange of the image plates, and an off-line image plate scanner. In a collaborative project between the EMBL Grenoble outstation and the ESRF, the EMBL is developing the image plate scanner and a robot assistant and the ID14 team is building the Weissenberg camera and the robot image plate changer.

THE CAMERA

The experimental station (Figure 1) is equipped with a four circle κ-diffractometer with a horizontal omega axis, a hood for P2 level biohazardous experiments covering the diffractometer, a tapered fibre optics coupled CCD detector on a 2θ arm, the Weissenberg camera with an optional helium chamber and a flat wall for holding the image plates. The wall can hold one or two 40 x 80 cm image plates, thus forming a maximum active area of 80 cm x 80 cm, or 8000 by 8000 pixels. Image plates and cassettes carry bar codes and their numbers are used in an image plate database. The database is linked to the camera, the scanner and the robot assistant, allowing fully automated image plate management during an experiment. With this set-up, many image plates are exposed as fast as possible without human intervention inside the hutch, and read off-line afterwards.

The image plate can be translated along any direction perpendicular to the X-ray beam. With the knowledge of the lattice, the cell dimensions, and the orientation of a crystal in the beam, optimal coupling constants between the Weissenberg translation and the spindle as well as the maximum oscillation range are calculated to avoid overlap of diffraction spots. This synchronisation of the two-dimensional Weissenberg motion and the spindle allows a more efficient use of the detector active area. Therefore a smaller number of oscillation frames is needed to collect a complete data set.

THE SCANNER

The scanner (Figure 2) is designed to read a number of image plates which are extracted automatically from a cassette holding up to sixteen 40 x 80 cm image plates. They are scanned on a cylindrical drum. Each image plate is picked up from the cassette with a suction cup, rolled onto the drum and held by vacuum. The relevant information of the image plate such as the status is checked with the database using the bar code. After scanning, the image plate is put back into the cassette and the image plate database is updated. This process is repeated until all the image plates are scanned.

During a scan, the drum rotates at 800 rpm while the read-out head moves

along the surface of the drum parallel to its axis. An incremental encoder on the drum drives a stepper motor translating the read-out head which is perfectly synchronised. The read-out head contains a 1" photo-multiplier tube (PMT) placed in front of the drum. The red light from a laser diode coming in at the side of the PMT is focused by a lens and reflected onto the drum by a small mirror placed near the centre of the filter in front of the PMT. A conical mirror is used to collect the 390 nm photostimulated blue light and the coloured glass filter stops the 680 nm red laser light.

The current from the photo-multiplier is sampled by a 16 bit analogue-to-digital converter (ADC) running at 2 MHz and is averaged for each pixel area. Pixel data are temporarily stored in a FIFO memory and sent through a dedicated ETHERNET link to a UNIX workstation. The electronics consists of three parts: a VME rack, an I/O interface board and a data acquisition board. The VME rack holds a VME CPU card with four I/O extension cards (2 digital I/O, 1 dual stepper motor, 1 FIFO memory (Designed by C. Herve, P. Chappelet, and F. Epaud, Computing Services, ESRF), the DC power supplies and the power cards for the stepper motors. A custom-made card next to the VME rack is used to interface the I/Os with the sensors and actuators and to perform hardware security protection using programmable logic devices. The data acquisition board with the ADC is located at the top of the scanner near the reading head and is galvanically isolated from the rest of the electronics. The drum is driven by an AC motor with a programmable power frequency generator.

Since the scanner is connected to a UNIX Workstation, the acquisition software has been developed in a Client Server architecture. On the VME side, the software is written in C++ on OS9 operating system. One client deals with the scan itself, communicates with a UNIX server to report the scanner activity and access the database. Another client is dedicated to the data transfer. On the UNIX side, a data transfer server stores the scanned data both in shared memory (for display) and as a file on a hard disk. Another server interfaces with the image plate database and with a GUI, written in Motif, which reports the scanner activity, and drives a display program. The scanner can also be used in manual mode (without the bar code reader and the database).

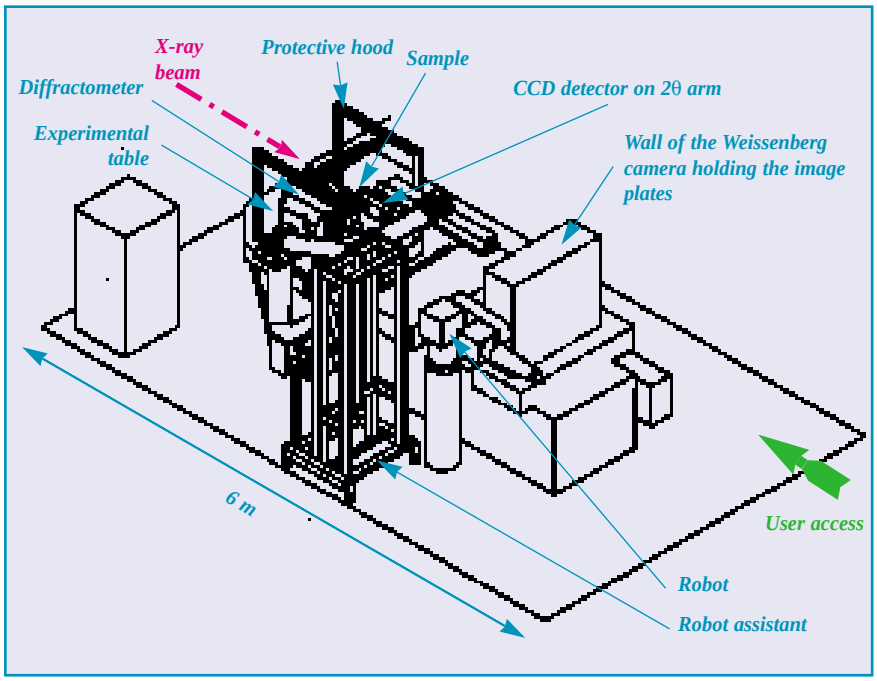

Fig. 1: The experimental station EH3 of ID14.

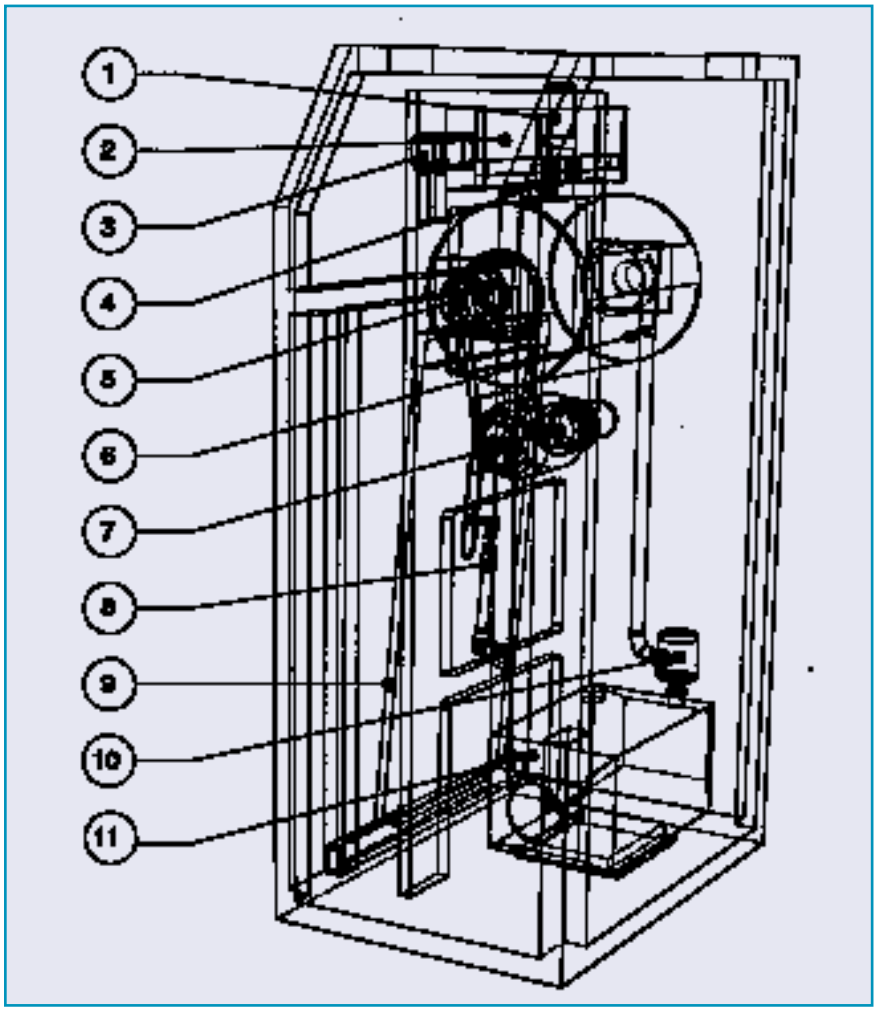

Fig. 2: The scanner. 1-Reading head 2-Head carrier 3-Head stepper motor 4-Laser diodes 5-Drum encoder 6-Drum and image plate 7-Drum AC scanning motor and stepper positioning motor 8-Image Plate transfer jacks 9-Image Plate cassette 10-Vacuum monitoring valves and pressure transducer 11-Vacuum pump.

MAIN CHARACTERISTICS (PRELIMINARY)

The scanner uses cassettes containing from 1 to 16 Fuji image plates (400 x 800 mm); the pixel size can be 100 or 200 μm^2; the scanning cycle time is 6 min 30 sec at 100 μm^2 and about 4 min at 200 μm^2 including the time for loading and unloading the image plates; the dynamic range is 16 bits; the noise is around 2-3 ADC unit (the gain is about one ^{55}Fe photon/ADC unit); the spatial resolution is 130 μm FWHM and about 800 μm FW1%M; the spatial distortion is below 50 μm; the absolute positional error of the plates is < 500 μm; image plates are identified with bar codes.

Figure 3 shows an image from a crystal of myrosinase taken on ID2 and scanned with 100 μm resolution.

Fig. 3: A diffraction image of a myrosinase crystal (space group C222, a = 137.0 Å, b = 139.2 Å, c = 82.1 Å) taken on ID2. Exposure time was 30 sec for a 1° oscillation. The image plate was scanned with 100 µm raster which gives 4000 pixels by 8000 pixels (64 Mbytes). The crystal-to-detector distance was 700 mm and the wavelength 0.988 Å.

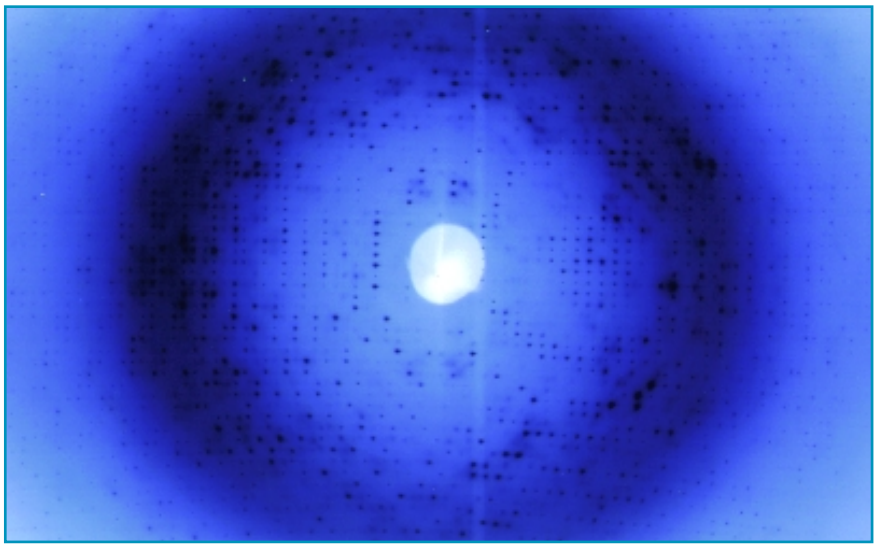

CONCLUSION AND FUTURE APPLICATIONS

Once operational, the image plate scanner, together with the rest of the data acquisition system, will provide a unique facility for collecting macromolecular crystallographic data from extremely large molecules. Using this set-up, it will be possible to screen good crystals from the crystallisation batches using the CCD detector, and, once finding a good one, to collect a complete data set using image plates before the crystal is damaged by the X-ray beam. This is especially relevant for virus crystals which often cannot be frozen and thus are subject to extensive radiation damages.

Another interesting application for the system is fast monochromatic time-resolved X-ray diffraction experiments. Here, rather wide oscillation ranges are used in order to collect a complete data set on one frame by translating the detector during the oscillation. Possible time resolution is expected to be of the order of a few minutes.

Two-Plane Focusing of 30 keV Undulator Radiation with a Refractive Lens

P. Elleaume,

ESRF, Machine Division

Recently a simple type of refractive lens has been proposed and successfully tested in the X-ray range with a photon energy of 14 keV [1]. Such lenses are made by drilling a series of small holes with a diameter of the order of a millimetre in a low Z material such as aluminium. These lenses are expected to be resistant to heatload and simple to build resulting in an astonishing low cost. Their drawbacks are their limitation to high photon energies above 4 keV due to absorption, their strong chromatic aberrations and low aperture. However they appear extremely well-suited to the focusing of the undulator radiation of the new hard X-ray third generation synchrotron sources such as the ESRF. The object of this paper is to report the results of some tests and to discuss the potentialities of these lenses.

Description of the Experiment

The original interest for these tests was the imaging of the electron beam sizes at the source of the undulator in the ID6 Machine Diagnostics beamline as a complementary emittance diagnostic. To do so, a lens was built by drilling 34 holes of 1 mm diameter with a vertical axis followed by 41 holes of the same diameter with an axis in the horizontal plane (see Figure 1). The holes are drilled in a 2 mm thick aluminium plate. As we shall see later, aluminium is not the best material but it was selected for its reasonably low Z, easy machining and short-term delivery. The vertical source size in the middle of the undulator is around 10 microns rms for the 40 pm emittance routinely achieved. For a proper magnification of the source, one needs to place the lens as close as possible to the source which conflicts with the severe heatload. In all cases water cooling is essential. The only places where sufficient water cooling is available on the ID6 beamline are the X-ray beam position monitor (xbpm) motorised stages called xbpm-1 and xbpm-2 located at a distance of 10.7 m and 22 m from the source. The design of the lenses was strongly inspired from the design of the tungsten blade of the xbpm [2] for which severe heatload problems have been carefully studied and solved. The shape of the lens is shown in Figure 1. The 8 lower large diameter holes are used for clamping. Of the 14.5 mm height of the lens, only the upper 5 mm emerge from the heavily cooled copper fastener. The entrance face of the lens is inclined at a low incidence angle to spread the heatload and reduce the temperature of the lens at the point of impact of the X-rays. To minimise the heatload issue, it was

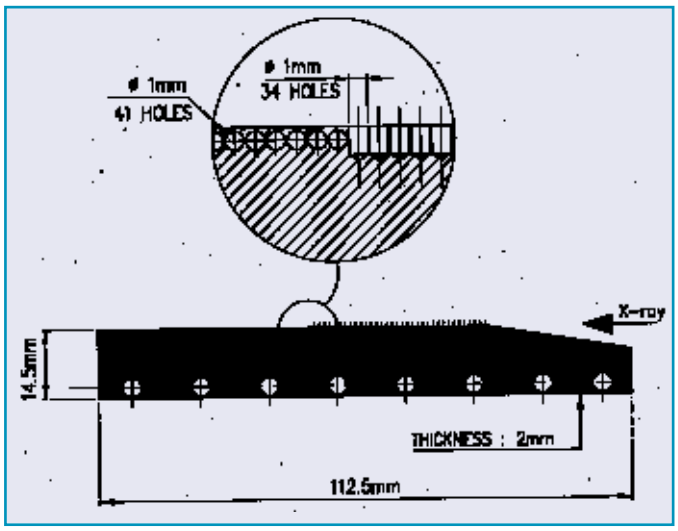

Fig. 1: Drawing of the two-plane refractive lens used in ID6. The input face is set at grazing angle to spread the heatload.

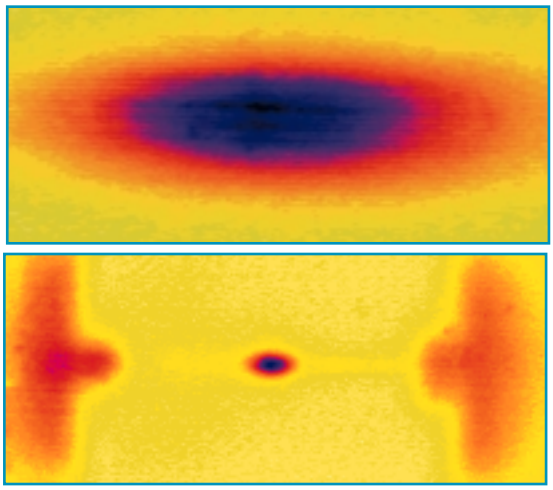

Fig. 2: Spot size of the seventh harmonic of the undulator at 29.5 keV observed at a distance of 32.2 m without lens. The rms sizes are 0.60 and 0.30 mm in good agreement with the emittance derived from the pinhole camera and the beta function of the source point.

decided to place the lens on xbpm-2 even though xbpm-1 would have been a better choice (size of image, spherical aberrations...). After passing through the lens the X-rays go through the graphite/beryllium window assembly placed in the front-end part of the beamline. The transmitted beam is then monochromatised by a 3 1 1 silicon crystal diffracting in the horizontal plane. The monochromatic beam is converted to visible light by means of a 1 mm thick CsI(Ti) scintillator and imaged by a CCD video-camera. The whole experiment was controlled and performed from the storage ring control room. The scintillator is placed at 32.2 m from the middle of the ID6 straight section. Such an imaging set-up has been in use for more than 4 years at the ID6 beamline and for more than two years as the primary emittance diagnostic of the electron beam [3]. The image of the X-ray beam when the monochromator is precisely tuned to the photon energy of one of the harmonics of the undulator spectrum on axis of the electron beam is essentially an intense ellipsoidal spot. This spot is the foot print of the undulator central cone on the scintillator. The focusing of the lens in both horizontal and vertical planes was selected for minimising the spot size of the image at a photon energy of 25 keV. A different number of holes was used for the focusing in the horizontal plane. This is due to the large beta function of the source (low divergence of the photon beam) responsible for a small violation of the geometrical optics laws (same as for visible lasers). The undulator used for this experiment is a single segment of 36 periods of 46 mm. The spectrum is tunable with a deflection parameter K between 0 and 2.2. The experiment has been performed at a full ring current of 200 mA with a gap ranging from 20 to 40 mm corresponding to a maximum angle integrated power of 1.7 kW and a normal incidence power density as high as 100W/mm^2 at the position of the lens.

RESULTS

Figure 2 presents the image of the 7th harmonic at a photon energy of 29.5 keV of the undulator before insertion of the lens. The rms horizontal and vertical sizes were measured to be 0.55 and 0.30 mm in good agreement with the beta function and emittance deduced from the pinhole camera [4]. The horizontal lines are produced by the unpolished beryllium window and graphite filters located 2 meters downstream from the lens. Figure 3 presents the same image after insertion of the lens and removing some attenuation. The central spot originates from the focusing of the lens in both the horizontal and vertical planes. As expected, the spot can be displaced on the camera by moving the lens and vanishes for large displacements of the lens due to stronger absorption in the aluminium. Table 1 summarises the measured rms sizes.

Fig. 3: Same image conditions as in Figure 2 after insertion of the lens and removal of some attenuation. The central spot is the result of the focusing of the radiation by the refractive lens. Some radiation is visible on the right and left hand side which is not passing through the lens.

These results are very encouraging. Horizontally the expected spot size is 0.11 mm. However, one would have expected a 0.010 mm rms vertical spot size around 25 keV. This discrepancy is not yet understood and several explanations are being studied such as the material inhomogeneity, aberration induced by the graphite and beryllium filters.

DISCUSSION

For a 30 keV radiation, the focal length of the lens is 12.2 m (10.2 m) in the horizontal (vertical) planes. As a result the corresponding apertures Σ are 0.18 mm (0.16 mm) to be compared with the rms beam size σ of the central cone of 0.45 mm (0.12) mm. The minimum thickness of aluminium is 0.1 x (34 + 41) + 4.2 = 11.7 mm. Consequently the overall transmission is 0.07 (material transmission) x 0.37 (horizontal aperture) x 0.81 (vertical aperture) = 0.021 which corresponds well to our observation. Derivation of the analytical expressions for the transmission of such lenses can be obtained from [5]. The rms aperture Σ of this lens is

$$\Sigma^2 = \frac{\delta}{4\pi\beta}\lambda F$$

where F is the focal, 1-δ and β are respectively the real part and imaginary part of the index of the material constituting the lens. If one replaces the aluminium with beryllium with the same hole radius and shape but a larger number of holes to achieve the same focal length, the overall transmission is 0.95, 0.75 and 0.4 at the photon energies of 30, 15 and 10 keV. In addition the temperature rise of the beryllium would be reduced due to its

Table 1: Measured rms photon beam size with and without the lens.

	Rms Horizontal Spot Size [mm]	Rms Vertical Spot Size [mm]
No Lens	0.55	0.30
29.5 keV	0.12	0.058
27.5 keV	0.11	0.056
25 keV	0.11	0.061

lower absorption. Other low Z materials are worth studying such as graphite, boron-nitride or boron-carbide. A lens made of beryllium would be almost absorption-free at any photon energy above 10 to 15 keV. A typical lens design for 1 to 1 imaging would need 60 times less holes than a lens design for a microfocus of say 30 to 1 ratio. This large difference comes both from the focal length required and from the positionning of the 1 to 1 lens at a shorter distance from the source allowing a smaller diameter for the hole. As a consequence of both the smaller number of holes and the longer focal distance, the 1 to 1 imaging lens is expected to have a much higher transmission and therefore efficiency. Such lenses could be very useful for a number of experiments. They could produce a vertical spot size of 10 microns rms on a sample placed at a 30 m distance from the source without modification of the divergence. Lower spot sizes are expected in the horizontal plane due to the higher emittance. Altogether, the spectral flux per unit surface on the sample at photon energies higher than 10 to 15 keV would therefore be more than 40 times higher than the present situation without affecting the divergence. Another important application of these lenses is in the use of the undulator spectrum without monochromator. The photon energy from each harmonic is focused differently. If one places a small aperture at the imaging plane of a specific harmonic, one would discriminate the other harmonics. The transmitted spectrum would be that of the selected harmonics with all the others attenuated. The lower the number of the selected harmonic the more efficient is the harmonic discrimination. The resulting number of photons per second per unit surface over a 1% bandwidth is several orders of magnitude higher than that presently achieved. Each lens is optimised for a specific photon energy, but operation over a large energy range can be achieved by installing an array of such lenses on a movable stage. A user would select a lens according to the application. The xbpm set-up presently in place in the ID6 beamline and optimised for a different goal (beam position measurement) allows the insertion of 4 different lenses without any modification. The power per unit surface on the sample or monochromator located at the image plane should not be significantly modified by the presence of the lens since only a small fraction of the spectrum is focused to a narrow size and a part of the power is deposited in the lens itself. Obviously to approach these performances, a number of issues need to be properly addressed such as the constraints induced by heatload, stability of the lens positioning system, required homogeneity and low rugosity of the low Z material etc.

CONCLUSION

Two-plane refractive lenses have a tremendous potentiality for a further optimisation of the undulator beamline of the ESRF. The potential improvement is so large that even if the ultimate performances are not reached, one could make use of imperfect lenses and still have a much higher spectral flux per unit surface without affecting the brilliance and the divergence of the radiation. ■

References

[1] A. Snigirev, V. Kohn, I. Snigireva & B. Lengeler, Nature Vol. 384, Nov. 7th, 1996.

[2] F. Loyer, DIPAC' 93 Conference , Montreux, Switzerland, May 93.

[3] E. Tarazona, P. Elleaume, Review of Scientific Instruments, Vol. 66, No.2, Feb. 1995.

[4] P. Elleaume, C. Fortgang, C. Penel, E. Tarazona, Journal of Synchr. rad. (1995). 2,209-214.

[5] P. Elleaume, ESRF Internal report ESRF / MACH ID 97/31

Nota Bene:
In the course of writing the paper, I have been informed that A. Snigirev achieved a 18 x 8 micro-meter spot size on a two-plane focusing lens at 30 keV with a focal length of 2 m made with 200 holes.

ACKNOWLEDGEMENTS

The author wishes to thank A. Snigirev for stimulating discussion, D. Gamonet and the Front-End Group who took care of the installation.

Events

February 1997
Visit of two French Ministers, Charles Millon and François d'Aubert

(see article on page 3)

April 1997
APS/SPring-8/ESRF workshop

(see article on page 3)

INTERNATIONAL CONFERENCE

Highlights in X-ray Synchrotron Radiation Research

17-21 November 1997
Grenoble (France)

(see details on page 6)

ORGANISED BY THE ESRF AND SPONSORED BY

The European Synchrotron Radiation Society • European Molecular Biology Laboratory, Grenoble • Antitron Technomedirad GmbH • CINEL s.r.l. Strumenti Scientifici • Hewlett Packard France and Summer System • Jobin Yvon-Spex Groupe Instruments S.A. • Métacéram S.A. • Micro-Controle Newport • SDMS S.A. • Sun Microsystems • Thomson Tubes Electroniques • Vacuum Generators • Varian S.A.

The ESRF Newsletter is published by the European Synchrotron Radiation Facility
BP 220, F38043 Grenoble cedex
Editor: Dominique CORNUÉJOLS Tél (33) 4 76 88 20 25

Dépôt légal : 2ème trimestre 1997. Printed in France by Repro-Express. Layout by Pixel Project.